Title
Neuronal activity regulates astrocytic Nrf2 signaling.

Journal
Proceedings of the National Academy of Sciences of the United States of America, 110(45)

ISSN
1091-6490

Authors
Habas, Agata
Hahn, Junghyun
Wang, Xianhong
et al.

Publication Date
2013-11-05

Peer reviewed

Neuronal activity regulates astrocytic Nrf2 signaling[1]

Agata Habas, Junghyun Hahn, Xianhong Wang and Marta Margeta*

Department of Pathology
University of California San Francisco, San Francisco, CA 94143

*Corresponding author:

UCSF Pathology, Box 0511
513 Parnassus Ave., HSW-514
San Francisco, CA 94143
Marta.Margeta@ucsf.edu
415-514-0228 (phone)
415-514-3165 (fax)

[1] **Non-standard abbreviations:** ACSF, artificial cerebrospinal fluid; 4-AP, 4-aminopyridine; AraC, cytosine arabinoside, ARE, Antioxidant Response Element; CaMKII, Ca^{2+}/calmodulin-dependent protein kinase II; Gab, gabazine (SR-95531); hPAP, human placental alkaline phosphatase; Keap1, Kelch-like ECH-associated protein 1; MAP2, microtubule-associated protein 2; mGluR, metabotropic glutamate receptor; NIM, nimodipine; Nrf2, nuclear factor erythroid 2-related factor 2**;** ROS, reactive oxygen species; SLF, sulforaphane.

Abstract

Nrf2, the transcriptional master regulator of the stress-induced antioxidant response, plays a key role in neuronal resistance to oxidative stress and glutamate-induced excitotoxicity. Nrf2-mediated neuroprotection is primarily conferred by astrocytes both *in vitro* and *in vivo*, but little is known about physiologic signals that regulate neuronal and astrocytic Nrf2 signaling. Here we report that activity of the Nrf2 pathway in the brain is fine-tuned through a regulatory loop between neurons and astrocytes: elevated neuronal activity leads to secretion of glutamate and other soluble factors, which activate the astrocytic Nrf2 pathway through a signaling cascade that involves group I metabotropic glutamate receptors and intracellular Ca^{2+}. Regulation of endogenous antioxidant signaling is a novel function of the neuron-astrocyte tripartite synapse; by matching the astrocyte neuroprotective capacity to the degree of activity in adjacent neuronal synapses, this regulatory mechanism may limit the physiologic costs associated with Nrf2 activation.

Significance

Tripartite synapse, which consists of presynaptic neuron, postsynaptic neuron, and perisynaptic astrocyte, is the central site of intercellular communication in the brain. Here, we show that neuron-astrocyte signaling at the tripartite synapse also regulates activity of Nrf2, the transcriptional master regulator of the stress-induced cytoprotective response: through secretion of neurotransmitter glutamate and other soluble messengers, elevated neuronal activity leads to increased expression of Nrf2-regulated genes in neighboring astrocytes. By optimizing astrocyte neuroprotective capacity to the level of adjacent synaptic activity, this regulatory mechanism may contribute to the maintenance of brain health under physiological stress.

Introduction

Nrf2, a basic leucine-zipper transcription factor, regulates both baseline and inducible expression of a battery of antioxidant and phase II detoxification enzymes (1). Under baseline conditions, Nrf2 is targeted for proteasomal degradation; stimuli that activate the Nrf2 pathway [oxidative stress, kinase activation, or treatment by small molecules such as sulforaphane (SLF)] lead to Nrf2 translocation into the nucleus and an increase in the transcription of genes that contain the ARE (Antioxidant Response Element) in the 5' regulatory region (2).

Nrf2 null mice develop diffuse white matter injury without overt loss of neurons (3). However, when these animals are exposed to mitochondrial toxins or oxidative stressors, they show increased susceptibility to neurodegeneration (4, 5). In cortical cultures, Nrf2 signaling is critical for neuronal resistance to mitochondrial complex I inhibitors, excessive Ca^{2+} influx, and glutamate-induced excitotoxicity (6). Interestingly, Nrf2-mediated neuroprotection is primarily conferred by astrocytes both *in vitro* (7, 8) and *in vivo*, where selective overexpression of Nrf2 under an astrocyte-specific promoter leads to increased survival in mouse models of

Parkinson's disease (9) and amyotrophic lateral sclerosis (10). However, little is known about physiologic signals that regulate Nrf2 signaling in the CNS.

Increased synaptic activity protects neurons from apoptosis induced by staurosporine (11) or oxidative stress (12) through upregulation of anti-apoptotic genes (13) and activation of intrinsic antioxidant defenses through FOXO, C/EBPβ and AP-1 signaling pathways (12). It is currently not known, however, whether increased synaptic activity can activate the Nrf2 pathway in either neurons or glia. Perisynaptic astrocytes, which together with pre- and postsynaptic neurons form a "tripartite synapse", regulate neuronal excitability and strength of synaptic transmission (14). Here, we show that neuron-astrocyte interactions also play a key role in the regulation of brain Nrf2 signaling.

Results

Neuronal activity potentiates Nrf2 signaling in mixed hippocampal cultures. To investigate whether Nrf2 signaling is regulated by neuronal activity, we used mixed and predominantly neuronal primary hippocampal cultures (Fig. 1A). Neuronal activity was induced by treatment with 50 mM K^+ (high K^+) artificial cerebrospinal fluid (ACSF), a commonly employed depolarizing stimulus that triggers a burst of action potentials and global neurotransmitter release (15). High K^+ treatment increased the level of nuclear 84 kDa Nrf2 protein in mixed, but not in neuronal or astrocytic cultures (Fig. 1B). In contrast, treatment with SLF (a direct activator of Nrf2 pathway) increased the nuclear Nrf2 protein in both mixed and astrocytic, but not in neuronal cultures (Fig. 1B). [Commercially available Nrf2 antibodies detect multiple protein bands, but only the 84 kDa band was increased by SLF treatment and attenuated by Nrf2 siRNA transfection in astrocyte cultures (Fig. S1A), indicating that it was specific for Nrf2. In all subsequent Western blotting experiments, SLF treatment was used as a positive control to unambiguously identify the specific Nrf2 band.]

Hippocampal cultures predominantly consist of excitatory glutamatergic neurons, but also contain a small number of GABAergic neurons that inhibit network activity (11). To investigate whether Nrf2 signaling can be activated through a local (synapse-restricted) neurotransmitter release, we treated cultures with $GABA_A$ receptor antagonist gabazine (Gab) and K^+ channel antagonist 4-aminopyridine (4-AP). Both Gab and 4-AP increase neuronal firing frequency and Ca^{2+} influx associated with activation of synaptic (but not extrasynaptic) NMDA receptors (NMDARs); combining the two drugs leads to a stronger response while preserving the high spatial specificity (11). Like high K^+, Gab/4-AP treatment increased nuclear Nrf2 protein level in mixed but not in neuronal or astrocytic cultures (Fig. 1C); weaker activation was seen when cultures were treated with either drug alone (Fig. S1B). Similar results were obtained with other $GABA_A$ receptor antagonists (bicuculline or picrotoxin; Figs. S1C and S1D). Interestingly, activation of Nrf2 signaling by Gab/4-AP required at least overnight treatment, while high K^+ was effective after as little as 2 h (Figs. S1E and S1F).

To confirm that increase in the nuclear Nrf2 protein level results in activation of downstream Nrf2 signaling, we used qRT-PCR to measure mRNA levels of a subset of Nrf2-regulated genes. In mixed cultures, both high K^+ and Gab/4-AP treatments increased levels of Nqo1 and Gclc mRNAs, while Ephx1 mRNA was increased only after high K^+ treatment (Figs. 1D and 1E).

In predominantly neuronal cultures, we measured a similar relative increase but smaller absolute levels for each mRNA (Fig. S2); given that neuronal cultures contain a small fraction of non-neuronal cells (Fig. 1A), these results suggest that neuronal firing increases Nrf2 activity in glia rather than neurons.

Neuronal activity activates Nrf2 signaling in astrocytes through (a) soluble factor(s). Mixed hippocampal cultures are primarily composed of neurons and astrocytes, but other glia are also present (Fig. 1A). To determine whether neurons and astrocytes are sufficient for Nrf2 activation by neuronal activity, we plated separately cultured astrocytes into AraC-treated neuronal cultures (Fig 2A). Treatment of these direct neuron-astrocyte co-cultures with high K^+ resulted in nuclear Nrf2 protein increase comparable to that seen in mixed cultures; no increase was observed in neuronal cultures that were not seeded with astrocytes (Fig. 2B). A similar result was seen if Gab/4-AP treatment was used to induce synaptic activity (Fig. 2C). In these experiments, neurons were cultured with astrocytes for 6 days prior to treatment; however, the same results were seen when the co-culture period was shortened to 1 day (Fig. S3).

To confirm that the Nrf2 pathway activation occurs in astrocytes rather than neurons (as suggested by results of qRT-PCR experiments), we used Gab/4-AP treatment to increase action potential frequency in brain slices from ARE-human placental alkaline phosphatase (hPAP) transgenic reporter mice (16) (Fig. S4). Both in control and Gab/4-AP-treated slices (Figs. 3A-C), hPAP-positive cells displayed characteristic astrocyte morphology [a small cell body with highly branched fine processes (17)]; no hPAP-positive cells with neuronal morphology (17) were observed (Fig. 3C). The number of hPAP-positive astrocytes was significantly higher in Gab/4-AP-treated than in vehicle-treated slices and was comparable to the number of hPAP-positive astrocytes in SLF-treated slices; importantly, Gab/4-AP effect was blocked by co-administration of voltage-gated Na^+ channel blocker tetrodotoxin (TTX), indicating that it was mediated by increased neuronal activity (Fig. 3D). In agreement with these results, siRNA-mediated Nrf2 knock-down in astrocytes attenuated the increase in nuclear Nrf2 protein level induced by either Gab/4-AP or high K^+ treatment in direct neuron-astrocyte co-cultures (Fig. S5).

To assess whether direct neuron-astrocyte contact was required for activation of astrocytic Nrf2 signaling by neuronal activity, we performed experiments in indirect neuron-astrocyte co-cultures, which allow preparation of separate lysate from each cell type. Following 4 h treatment with high K^+, nuclear Nrf2 protein level was increased in astrocytes co-cultured with neuronal inserts but not in neurons co-cultured with astrocyte inserts (Fig. 3E), indicating that neuronal activation of the astrocytic Nrf2 pathway is mediated by (a) diffusible messenger(s). Next, we examined whether Nrf2 signaling in astrocytes can be activated by high K^+ ACSF pre-conditioned on AraC-treated neurons (NC-high K^+); as a control, we treated astrocytes with regular high K^+ ACSF. Surprisingly, nuclear Nrf2 was not increased in astrocytes treated for 4 h with NC-high K^+ (Fig. 3F). In this experiment, both neurons and astrocytes were “naïve” (i.e. cultured separately), raising the possibility that co-culturing neurons and astrocytes in the same medium for several days (as done in the insert experiments) leads to neuron and/or astrocyte changes that enable Nrf2 induction by neuronal activity. To examine this possibility, we cultured astrocytes with neuronal inserts and neurons with astrocyte inserts for 3 days prior to ACSF

conditioning and astrocyte treatment. As in the experiment with naïve neurons and astrocytes (Fig. 3F), there was no increase in nuclear Nrf2 following treatment with NC-high K^+ (Fig. 3G).

Nrf2 activation requires mature synapses and depends on glutamatergic and Ca^{2+}signaling. To examine whether activity-mediated upregulation of the Nrf2 pathway requires fully mature synapses, we performed experiments in mixed cultures at different stages of maturity. Gab/4-AP treatment activated Nrf2 signaling at DIV14 but had no effect at DIV3 or DIV7, suggesting that mature synapses [which form after 10 days *in vitro* (18)] are required for Nrf2 activation (Fig. S6A). To exclude the possibility that the lack of Gab/4-AP effect in early cultures was due to low astrocyte-neuron ratio, we performed the same experiment using high K^+ treatment (which does not depend on fully mature synapses for its efficacy). In contrast to Gab/4-AP treatment, high K^+ treatment led to a similar increase in nuclear Nrf2 protein level at all culture ages (Fig. S6B), indicating that the number of astrocytes in early cultures was sufficient for Nrf2 activation.

Hippocampal cultures are primarily composed of glutamatergic neurons. To determine whether Nrf2 activation in astrocytes is mediated by neuronally-secreted glutamate, mixed cultures were treated with TTX, glutamate receptor antagonists, extracellular Ca^{2+} chelator EGTA, or intracellular Ca^{2+} chelator BAPTA-AM prior to induction of neuronal activity. When mixed cultures were treated with Gab/4-AP to selectively increase synaptic activity, increase in nuclear Nrf2 was fully or almost fully blocked by TTX, EGTA and BAPTA (Figs. 4A and S7A-B). In contrast, partial block was seen with NMDAR antagonists MK801 and APV, nonselective mGluR antagonist MCPG, and AMPAR antagonists NBQX and CNQX. The results were slightly different when high K^+ treatment was used to increase global neuronal activity (Figs. 4B and S7C). As expected, under these conditions Nrf2 activation was largely unaffected by TTX treatment; in contrast, chelation of either extracellular or intracellular Ca^{2+} completely blocked Nrf2 upregulation. The effect of glutamate receptor antagonists was more equivocal: partial block was seen with nonselective mGluR antagonist MCPG but not with group II/III mGluR antagonist LY341495; ionotropic glutamate receptor antagonists NBQX, CNQX, APV and MK801 were largely without effect. Finally, L-type Ca^{2+} channel blocker nimodipine had no effect on Nrf2 activation by high K^+ treatment. While these results suggest that neuronal regulation of astrocytic Nrf2 activity is complex, it clearly depends on neuronal firing, intracellular Ca^{2+}, and glutamate receptor signaling.

To further investigate the role of glutamate receptors in the regulation of the astrocytic Nrf2 pathway, we treated astrocyte cultures with glutamate, NMDA, or DHPG (group 1 mGluR agonist). In the majority of our experiments, these treatments had no effect on nuclear Nrf2 level (Fig. 4C), although a small increase in nuclear Nrf2 was sometimes seen following glutamate and DHPG (but not NMDA) treatments (Fig. S7D). Finally, astrocyte cultures were treated with glutamate in high K^+ or control ACSF to investigate whether Nrf2 upregulation requires glutamate receptor activation concurrent with astrocyte depolarization. Surprisingly, nuclear Nrf2 level was lower in astrocytes treated with glutamate-ACSF than in astrocytes treated with ACSF alone (Fig. 4D). Importantly, however, there was no difference in nuclear Nrf2 level between astrocytes treated with glutamate in control or high K^+ ACSF, suggesting that astrocyte depolarization has no effect on Nrf2 activity. Taken together, these data indicate that glutamate receptor activation is necessary but not sufficient for Nrf2 activation by neuronal activity.

Discussion

Neuronal susceptibility to injury critically depends on Keap1/Nrf2/ARE signaling, but little is known about physiologic signals that regulate this neuroprotective pathway in the CNS. Our experiments showed that both depolarization-induced global neurotransmitter release and increased endogenous synaptic activity lead to Nrf2 activation in the mixed neuron-glia environment, but have little effect on Nrf2 signaling in predominately neuronal cultures (Fig. 1). Furthermore, we found that activity-mediated regulation of Nrf2 requires neurons and astrocytes, but not other types of glia (Fig. 2) and that activity-induced potentiation of Nrf2 signaling is restricted to astrocytes, with no upregulation seen in neurons (Fig. 3). These findings are consistent with the previous work, which showed (i) that, based on gene expression profiling, activation of synaptic NMDAR in neuronal cultures does not lead to induction of classic Nrf2-regulated genes (12); and (ii) that activity-dependent induction of sulfiredoxin in neuronal cultures is largely independent of Nrf2, although this gene can be upregulated in neurons by treatment with pharmacologic Nrf2 inducers (19).

Astrocytic Nrf2 signaling was upregulated in response to elevated neuronal activity in intact brain slices (Figs. 3A-D), direct co-cultures (which allow extensive intercellular contacts; Figs. 2 and S5) and indirect co-cultures (in which the two cell types share the same medium but are divided by a physical gap; Fig. 3E). These findings suggest that increased neuronal activity is conveyed to perisynaptic astrocytes through one or more soluble factors secreted by neurons. Surprisingly, however, there was no increase in astrocytic Nrf2 signaling in response to neuronally-conditioned high K^+ ACSF (Figs. 3F and 3G). There are two possible explanations for this discrepancy: (i) neuronally-secreted factors required for Nrf2 induction are chemically unstable and thus not present at a sufficient concentration in the NC-ACSF, or (ii) neuronal activation of the astrocytic Nrf2 pathway requires bidirectional signaling between neurons and astrocytes.

What is the nature of soluble messengers that mediate neuronal activation of astrocytic Nrf2 signaling? When Nrf2 activation is induced by Gab/4-AP treatment, it requires a well-developed synaptic network, action potential firing, and NMDAR, AMPAR, and mGluR activity (Figs. S6A, 4A, and S7A). In contrast, Nrf2 activation by high K^+ treatment is seen in immature cultures with incompletely developed synapses, does not require action potential firing, and depends on metabotropic but not ionotropic glutamate receptor signaling (Figs. S6B, 4B, and S7C). These differences are consistent with the mechanism of action described for each treatment: while Gab/4-AP leads to network disinhibition and consequent increase in endogenous synaptic activity, high K^+ causes action potential-independent global neurotransmitter release. Irrespective of these differences, Nrf2 activation by either treatment was partly blocked by one or more glutamate receptor antagonists, indicating that neuronally-secreted glutamate plays an important role in the neuronal regulation of the astrocytic Nrf2 pathway. Surprisingly, however, direct glutamate treatment was largely without an effect on astrocytic Nrf2 signaling (Fig. 4C), with weak activation observed only in a subset of experiments (Fig. S7D); this finding is consistent with the lack of Nrf2 activation by NC-ACSF, which presumably contains abundant glutamate released from presynaptic neurons during the conditioning step (Figs. 3F and 3G).

Nrf2 activation by Gab/4-AP was blocked by antagonists of both ionotropic (NMDAR and AMPAR) and metabotropic glutamate receptors; in contrast, only the nonselective mGluR

antagonist MCPG (but not the selective mGluR group II antagonist LY341495) partially inhibited Nrf2 activation by high K^+ (Figs. 4 and S7). Together with weak activation of astrocytic Nrf2 signaling induced by mGluR group I agonist DHPG in a subset of experiments (Fig. S7D), these data suggest that glutamate released by presynaptic neurons activates astrocytic Nrf2 signaling by acting on astrocytic group I mGluRs (mGluR1 and/or mGluR5), which couple to G_q G protein and lead to an increase in the intracellular Ca^{2+}. Ionotropic glutamate receptors, on the other hand, play a significant role only in the Nrf2 activation by synapse-dependent Gab/4-AP treatment. Together with the lack of Nrf2 activation following direct NMDA treatment of astrocytes (Figs. 4C and S7D), this finding suggests that ionotropic glutamate receptors act indirectly – at presynaptic and/or postsynaptic termini – by regulating neuronal release of glutamate and/or other secreted messengers that mediate Nrf2 activation. Collectively, these data suggest that neuronal activation of the glial Nrf2 pathway requires presynaptically-released glutamate acting in combination with other factor(s) secreted by the presynaptic neuron, postsynaptic neuron, or even the perisynaptic astrocyte in an auto-regulatory feedback loop (Fig. 5); an interesting candidate for this role is superoxide anion, which is produced by neuronal NADPH oxidase in response to NMDAR activation and leads to oxidative stress in neighboring neurons and astrocytes (20).

The Nrf2 pathway can be activated through phosphorylation of Nrf2 itself or through oxidation of cysteine residues on its cytoplasmic regulator, Keap1 (21). Downstream of Ca^{2+}, the signal transduction pathway for Nrf2 activation thus might include Ca^{2+}-dependent kinases (such as PI3K, CaMKII, or PKC) and/or astrocytic NADPH oxidase, which produces ROS in response to a rise in the cytosolic Ca^{2+} (22). While canonical regulation of Nrf2 activity is post-translational (2), neuronal activation of astrocytic Nrf2 signaling may also include transcriptional mechanisms: in contrast to SLF treatment, which does not alter neuronal activity (Figs. S4C-D), both high K^+ and Gab/4-AP treatments increased Nrf2 mRNA level in mixed cultures (Figs. S8A); neither treatment directly altered proteasome activity (Figs. S8C). Interestingly, not all stimuli that elevate cytosolic Ca^{2+} in astrocytes lead to Nrf2 pathway activation: treatment of astrocyte cultures with high K^+ in the absence of neurons led to a small increase in Nrf2 mRNA level (Fig. S8B) but did not result in an increase in the nuclear Nrf2 protein level (Figs. 1B, 3F, 3G, and 4D). Thus, either cytosolic Ca^{2+} has to be elevated within a specific signaling compartment or Nrf2 pathway activation requires simultaneous activation of two or more signaling cascades.

What is the functional significance of neuronal regulation of glial Nrf2 signaling? Elevated Nrf2 activity in astrocytes protects neurons both *in vitro* (7, 8) and *in vivo* (9, 10), and has been shown to contribute to the neuroprotective effect of ischemic preconditioning (23). Through the regulatory mechanism we uncovered, the level of Nrf2 activity in a perisynaptic astrocyte is matched to the degree of activity in the adjacent synapse (Fig. 5). Under physiologic conditions (modeled by Gab/4-AP treatment), high-activity synapses are afforded greater neuroprotection than the low activity ones; by restricting Nrf2 upregulation only to active synapses, this regulatory feedback loop may compartmentalize effects of Nrf2 activation on the redox-sensitive signaling pathways. Under pathologic conditions (modeled by high K^+ treatment), the synapse specificity will be lost in favor of a greater and more rapid (Figs. S1E-F) Nrf2 activation; the globally elevated Nrf2 activity will protect the entire neuronal field at risk, albeit with possibly significant physiologic costs.

In conclusion, the activity of Keap1/Nrf2/ARE neuroprotective pathway in the CNS is fine-tuned through a regulatory loop between neurons and astrocytes: neuronal firing leads to secretion of glutamate and other (still unidentified) soluble factors, which activate the astrocytic Nrf2 pathway through a signaling cascade that involves group I mGluRs and intracellular Ca^{2+}. Uncovering the details of this regulatory pathway thus has the potential to foster development of pharmacologic treatments that will provide neuroprotection in a synapse and/or neuron-specific manner.

Materials and Methods

Additional experimental details (including description of Western blotting, qRT-PCR, siRNA transfection, proteasome assay, electrophysiology, hPAP histochemistry, and immunocytochemistry protocols) are provided in the SI Material. The use and care of animals followed the guideline of the Institutional Animal Care and Use Committee at University of California, San Francisco.

Primary mixed, neuronal, and astrocytic cultures. Primary hippocampal cultures were prepared from E19 embryos obtained from timed-pregnant Sprague-Dawley rats (Charles River). Following tissue dissociation, cells were cultured for 2-3 weeks prior to experiments (unless otherwise indicated). To obtain predominantly neuronal cultures, a subset of cultures was treated with 1 μM AraC at DIV3 to prevent glial cell proliferation; mixed cultures were left untreated. Primary hippocampal or mixed hippocampal/cortical astrocytic cultures were prepared from E19 or E21 embryos; one week after plating, cultures were vigorously shaken overnight to remove microglia and oligodendroglia. In all experiments, each biological replicate was performed in a different culture batch.

Direct neuron-astrocyte co-cultures. DIV14-28 astrocytes were plated into AraC-treated neuronal cultures (DIV10 or DIV13-14) at a density of ~ 1.7×10^4 cells/cm^2; experiments were done at neuronal culture DIV14-16 (i.e. either 1 or 6 days after establishment of co-cultures).

Indirect neuron-astrocyte co-cultures. Neurons and astrocytes were cultured either in 6-well tissue culture plates or on inserts designed to fit them; this experimental set-up prevents direct cell-to-cell contact but allows exchange of soluble messengers. At neuronal culture DIV14, two culture configurations were established in neuronal maintenance medium (to mimic mixed culture conditions): (1) astrocyte inserts were placed on top of neuronal cultures and (2) neuronal inserts were placed on top of astrocytic cultures. Experiments were performed 3 days later; following treatment, only cells cultured on the bottom of 6-well plates were collected for fractionation and Western blotting (cell yield from inserts was too low to obtain an adequate amount of protein). In all experiments, neuronal and mixed cultures from the same batch were used as negative and positive controls, respectively.

Quantification of hPAP-positive cells. 400 μM thick coronal brain slices from 17 P21-26 ARE-hPAP transgenic mice were treated for 48 h with 0.1% DMSO, 20 μM Gab + 2.5 mM 4-AP, 20

μM Gab + 2.5 mM 4-AP + 1 μM TTX, or 2.5 μM SLF, and then fixed, cryoprotected, and cut into 20 μM sections for hPAP histochemistry. hPAP-positive cells were counted over the entire section (4-8 sections / treatment slice; 1 slice per animal for each treatment), with Kruskal-Wallis one-way ANOVA on ranks used for statistical analysis.

High K^+ treatment and preconditioning. Regular ACSF (145.5 mM NaCl, 2.5 mM KCl, 1 mM $MgCl_2$, 10 mM HEPES-NaOH, 10 mM glucose, 2 mM $CaCl_2$; pH 7.4) and high K^+ ACSF (98 mM NaCl, 50 mM KCl, 1 mM $MgCl_2$, 10 mM HEPES-NaOH,10 mM glucose, 2 mM $CaCl_2$; pH 7.4) solutions were prepared fresh before each treatment. In the first set of preconditioning experiments, "naïve" DIV16-17 neurons (never cultured with astrocytes) were treated with control or high K^+ ACSF solution for 10 min or 4 h; preconditioned solutions were then used to treat "naïve" astrocytes (never cultured with neurons) for 4 h, with non-preconditioned ACSF solutions used as a negative control. In the second set of preconditioning experiments, neurons were co-cultured with astrocyte inserts and astrocytes with neuronal inserts for 3 days. After insert removal, neurons were treated with control or high K^+ ACSF solution for 10 min; preconditioned solutions were used to treat astrocytes for 4 h.

Acknowledgments

This work was supported by UCSF Program for Breakthrough Scientific Research Start-up Award, UCSF Academic Senate Start-up Award, and NIH grants NS054113 and NS073765, all to MM. We are grateful to Dr. Jeffrey Johnson (University of Wisconsin) for the gift of ARE-hPAP mice, Ms. Natasha Chandiramani for help with early experiments, and Ms. Christine Lin for aid with figure preparation.

References

1. Kensler TW, Wakabayashi N, Biswal S (2007) Cell survival responses to environmental stresses via the Keap1-Nrf2-ARE pathway. *Annu Rev Pharmacol Toxicol* 47:89-116.
2. Zhang DD (2006) Mechanistic studies of the Nrf2-Keap1 signaling pathway. *Drug Metab Rev* 38:769-789.
3. Hubbs AF*, et al.* (2007) Vacuolar leukoencephalopathy with widespread astrogliosis in mice lacking transcription factor Nrf2. *Am J Pathol* 170:2068-2076.
4. Burton NC, Kensler TW, Guilarte TR (2006) In vivo modulation of the Parkinsonian phenotype by Nrf2. *Neurotoxicology* 27:1094-1100.
5. Shih AY*, et al.* (2005) Induction of the Nrf2-driven antioxidant response confers neuroprotection during mitochondrial stress *in vivo*. *J Biol Chem* 280:22925-22936.
6. Lee JM, Shih AY, Murphy TH, Johnson JA (2003) NF-E2-related factor-2 mediates neuroprotection against mitochondrial complex I inhibitors and increased concentrations of intracellular calcium in primary cortical neurons. *J Biol Chem* 278:37948-37956.
7. Kraft AD, Johnson DA, Johnson JA (2004) Nuclear factor E2-related factor 2-dependent antioxidant response element activation by *tert*-butylhydroquinone and sulforaphane occurring preferentially in astrocytes conditions neurons against oxidative insult. *J Neurosci* 24:1101-1112.
8. Shih AY*, et al.* (2003) Coordinate regulation of glutathione biosynthesis and release by Nrf2-expressing glia potently protects neurons from oxidative stress. *J Neurosci* 23:3394-3406.

9. Chen PC*, et al.* (2009) Nrf2-mediated neuroprotection in the MPTP mouse model of Parkinson's disease: Critical role for the astrocyte. *Proc Natl Acad Sci U S A* 106:2933-2938.
10. Vargas MR, Johnson DA, Sirkis DW, Messing A, Johnson JA (2008) Nrf2 activation in astrocytes protects against neurodegeneration in mouse models of familial amyotrophic lateral sclerosis. *J Neurosci* 28:13574-13581.
11. Hardingham GE, Fukunaga Y, Bading H (2002) Extrasynaptic NMDARs oppose synaptic NMDARs by triggering CREB shut-off and cell death pathways. *Nat Neurosci* 5:405-414.
12. Papadia S*, et al.* (2008) Synaptic NMDA receptor activity boosts intrinsic antioxidant defenses. *Nat Neurosci* 11:476-487.
13. Zhang SJ*, et al.* (2007) Decoding NMDA receptor signaling: identification of genomic programs specifying neuronal survival and death. *Neuron* 53:549-562.
14. Fields RD, Stevens-Graham B (2002) New insights into neuron-glia communication. *Science* 298:556-562.
15. Bading H, Ginty DD, Greenberg ME (1993) Regulation of gene expression in hippocampal neurons by distinct calcium signaling pathways. *Science* 260:181-186.
16. Johnson DA, Andrews GK, Xu W, Johnson JA (2002) Activation of the antioxidant response element in primary cortical neuronal cultures derived from transgenic reporter mice. *J Neurochem* 81:1233-1241.
17. Murphy TH*, et al.* (2001) Preferential expression of antioxidant response element mediated gene expression in astrocytes. *J Neurochem* 76:1670-1678.
18. Nwabuisi-Heath E, Ladu MJ, Yu C (2012) Simultaneous analysis of dendritic spine density, morphology and excitatory glutamate receptors during neuron maturation in vitro by quantitative immunocytochemistry. *J Neurosci Methods* 207:137-147.
19. Soriano FX*, et al.* (2008) Induction of sulfiredoxin expression and reduction of peroxiredoxin hyperoxidation by the neuroprotective Nrf2 activator 3H-1,2-dithiole-3-thione. *J Neurochem* 107:533-543.
20. Reyes RC, Brennan AM, Shen Y, Baldwin Y, Swanson RA (2012) Activation of neuronal NMDA receptors induces superoxide-mediated oxidative stress in neighboring neurons and astrocytes. *J Neurosci* 32:12973-12978.
21. Kaspar JW, Niture SK, Jaiswal AK (2009) Nrf2:INrf2 (Keap1) signaling in oxidative stress. *Free Radic Biol Med* 47:1304-1309.
22. Abramov AY*, et al.* (2005) Expression and modulation of an NADPH oxidase in mammalian astrocytes. *J Neurosci* 25:9176-9184.
23. Bell KF*, et al.* (2011) Mild oxidative stress activates Nrf2 in astrocytes, which contributes to neuroprotective ischemic preconditioning. *Proc Natl Acad Sci U S A* 108:E1-2.

Figure Legends

Fig.1. High K^+ and Gab/4-AP treatments activate Nrf2 signaling in mixed hippocampal cultures. (A) Neuronal, mixed, and astrocytic cultures were immunostained for Map2 (neuronal marker, green) and GFAP (astrocytic marker, red); DAPI nuclear staining (blue) was used to visualize all cells. At DIV14, mixed cultures were composed of 49±9% neurons, 17±2% astrocytes and 33±11% other cells (presumably oligodendroglia and microglia), while AraC-treated, neuron-enriched cultures consisted of 95±2% neurons, 4±2% astrocytes, and 1±1% other cell types (mean±SD, n=3). In astrocytic cultures, no neurons were present and nearly all nuclei were associated with GFAP-positive cell bodies. Note that astrocytes cultured with neurons extend many long processes, while astrocytes cultured alone exhibit a flat, epithelioid morphology. Scale bar, 50 µm. **(B and C)** Neuronal, mixed, and astrocytic cultures were treated with control or 50 mM K^+ ($\uparrow K^+$) ACSF for 4 h (B), 0.1% DMSO (Veh) or 20 µM Gab + 2.5 mM 4-AP (Gab/4-AP) for 24 h (C), or 2.5 µM SLF for 16 h (B and C). Nuclear Nrf2 protein level

(apparent MW: 84 kDa) was increased by high K^+ and Gab/4-AP treatments only in mixed cultures. Cytosolic Nrf2 protein level was generally below the detection threshold; however, an increase in cytosolic Nrf2 was occasionally seen in SLF-treated astrocytic cultures (C). Representative of 5 or more similar experiments are shown. **(D and E)** Mixed cultures were treated with control or high K^+ ACSF for 4 h (D) or with 0.1% DMSO (Veh) or Gab/4-AP for 24 h (E). A statistically significant increase in Nqo1 and Gclc mRNA was seen with both treatments, while only high K^+ treatment led to increase of Ephx1 mRNA; the level of Gclm mRNA was not significantly changed after either treatment. Note that both baseline and induced levels for all mRNAs (except Gclm) were lower in ACSF than in the culture medium, which was used for Gab/4-AP treatment. *, $p<0.05$; **, $p<0.01$ (mean±SEM, two-tailed t-test, n=5).

Fig. 2. Nrf2 pathway activation by high K^+ or Gab/4-AP requires neurons and astrocytes. Direct neuron-astrocyte co-cultures were obtained by plating astrocytes into DIV10 neuronal cultures, with experiments performed 6 d after astrocyte plating. **(A)** Mixed cultures, neuronal cultures, and direct neuron-astrocyte co-cultures were immunostained for Map2 and GFAP as in Fig. 1; DAPI nuclear staining (blue) was used to visualize all cells. A representative of 3 experiments is shown; scale bar, 50 μm. **(B and C)** Culture treatments were performed as described in Fig. 1 legend. Nuclear Nrf2 protein level was increased by high K^+ and Gab/4-AP treatments to a similar extent in mixed cultures and direct neuron-astrocyte co-cultures; representative of 3 or more similar experiments are shown.

Fig. 3. Neuronal activity induces Nrf2 signaling in astrocytes through a diffusible messenger. (A-C) Following Gab/4-AP treatment, hPAP-positive cells (arrow in C) showed astrocytic morphology (A and B, frontal cortex; C, hippocampus); neurons were not hPAP-positive (arrowheads in C mark the two blades of the dentate gyrus, which contain granule neurons). Scale bars: A and B, 200 μM; C, 40 μM. **(D)** The number of hPAP-positive astrocytes was significantly higher in Gab/4-AP-treated than control and Gab/4-AP+TTX-treated slices, but similar to SLF-treated slices (**, $p<0.01$; n=17, Kruskal-Wallis ANOVA on ranks). The data were not normally distributed and are represented as statistical box charts (horizontal lines: 25^{th}, 50^{th} and 75^{th} percentiles; error bars: 5^{th} and 95^{th} percentiles). **(E)** Cultures were treated as described in Fig. 1C legend. Following high K^+ treatment, nuclear Nrf2 protein was elevated in astrocytes that were co-cultured with neuronal inserts, but not in neurons that were co-cultured with astrocyte inserts; a representative of at least 3 similar experiments is shown. **(F)** Astrocytes were treated with either regular or neuronally-preconditioned (NC-) ACSF solutions for 4 h. Irrespective of the length of the conditioning step, there was no increase in nuclear Nrf2 in response to NC-high K^+; 16 h treatment with SLF was used as a positive control. A representative of at least 3 similar experiments is shown. **(G)** Experiment was performed as in (F), except that neurons were co-cultured with astrocyte inserts and astrocytes with neuron inserts for 3 days prior to insert removal, ACSF preconditioning, and astrocyte treatment. Again, there was no increase in nuclear Nrf2 in astrocytes treated for 4 h with NC-high K^+. A representative of at least 3 similar experiments is shown.

Fig. 4. Nrf2 activation depends on glutamatergic signaling and requires Ca^{2+}. (A) Nrf2 activation by synaptic activity was attenuated following neuronal silencing, block of metabotropic and ionotropic glutamate receptors, and chelation of extracellular Ca^{2+}. Mixed cultures were

treated for 24 h with Gab/4-AP alone or with 200 μM APV, 10 μM MK801, 1 μM TTX, 50 μM MCPG, 10 μM NBQX, 10 μM CNQX, 50 μM MCPG + 200 μM APV, or 1 mM EGTA; 24 h treatment with 0.2% DMSO (Veh) was used as a negative and 16 h treatment with 2.5 μM SLF as a positive control. Representatives of 4 or more similar experiments are shown; for another example, see Figs. S7A-B. **(B)** Nrf2 activation by global neuronal depolarization was attenuated following block of metabotropic (but not ionotropic) glutamate receptors and chelation of Ca^{2+}. Mixed cultures were treated for 4 h with high K^+ ACSF alone or in combination with 1 μM TTX, 10 μM nimodipine (NIM), 10 μM MK801, 200 μM APV, 1 mM EGTA, 250 μM MCPG, 1 μM LY341495 (a selective mGluR group II/III antagonist), 10 μM NBQX, or 10 μM CNQX; 4 h treatment with control ACSF was used as a negative and 16 h treatment with 2.5 μM SLF as a positive control. In BAPTA-AM experiments, cultures were pre-treated with 50 μM BAPTA-AM for 30 min, washed, and then treated with high K^+ ACSF. Representatives of 3 or more similar experiments are shown; for another example, see Fig. S7C. **(C)** Astrocytes were treated for 16 h with 0.1% DMSO (Veh), 2.5 μM SLF, 300 μM glutamate (Glu), 300 μM NMDA, 10 μM DHPG (a selective mGluR group I agonist), 300 μM NMDA + 10 μM DHPG, or 300 μM Glu + 1 mM EGTA (all in culture medium); Glu or NMDA treatments were combined with 30 μM glycine, which is NMDAR co-agonist. There was no increase in nuclear Nrf2 level in response to glutamate or its analogs; this outcome was seen in 4 of 6 similar experiments. Weak activation by Glu and DHPG, but not NMDA, was seen in 2 of 6 experiments (Fig. S7D). **(D)** Astrocytes were treated for 4 h with control or high K^+ ACSF either alone or in combination with 300 μM Glu and 30 μM glycine; 16 h treatment with 2.5 μM SLF was used as a positive control. Nuclear Nrf2 level was lower in astrocytes treated with glutamate-ACSF than in astrocytes treated with ACSF alone, but there was no difference between astrocytes treated with glutamate in control or high K^+ ACSF. A representative of 4 similar experiments is shown.

Fig. 5. Model for regulation of Nrf2 signaling at tripartite neuron-astrocyte synapse. At a low activity synapse **(A)**, glutamate secreted by presynaptic terminus (red arrow) mildly activates Nrf2 signaling in adjacent astrocytes through mGluR1/5 and Ca^{2+}-dependent pathway. At a high activity synapse **(B)**, increased secretion of glutamate and other (currently unidentified) soluble factor(s) secreted by a presynaptic neuron (brown arrow), postsynaptic neuron (blue arrow), and/or astrocyte itself (green arrow) strongly activate astrocytic Nrf2 signaling. This regulatory mechanism matches Nrf2 activity in a perisynaptic astrocyte to the firing rate of the adjacent neuronal synapse, maximizing the neuroprotection while minimizing the associated physiologic costs.

Supplemental Materials and Methods

Primary hippocampal mixed and neuronal cultures. Primary hippocampal cultures were prepared from E19 embryos obtained from timed-pregnant Sprague-Dawley rats (Charles River). After removal, brains were placed in a slice dissection solution (SLDS, 82 mM Na_2SO_4, 30 mM K_2SO_4, 10 mM HEPES, 10 mM glucose, 5 mM $MgCl_2$, pH = 7.4). Hippocampi were isolated with the aid of a dissection microscope, incubated in protease 23 diluted in SLDS (3 mg/ml; Sigma) for 15 minutes at 37°C, washed 2 times in plating medium [10% heat inactivated FBS (Omega Scientific or Gibco), 0.45% glucose, 0.11 mg/ml sodium pyruvate, 200 mM L-glutamine, 10 µg/mL penicillin, and 10 units/mL streptomycin in Eagle's MEM with Earles' BSS without L-glutamine], and then mechanically dissociated in the plating medium by trituration. Following dissociation, cells were plated (at a density of ~ 6.7 x 10^4 cells/cm^2) in tissue culture dishes previously coated with 0.1 mg/mL poly-L-lysine (Sigma) and then cultured in a humidified atmosphere of 95% air and 5% CO_2. Two to 16 h after plating, the plating medium was replaced with the maintenance medium [B27 supplement (Invitrogen), 0.5 mM L-glutamine, 10 µg/mL penicillin, and 10 units/mL streptomycin in Neurobasal medium (Invitrogen)]. To obtain predominantly neuronal cultures, cells were treated with 1 µM AraC (Sigma) at DIV3 to prevent glial cell proliferation; mixed cultures were left untreated. Half of the medium in both cultures was replaced with fresh medium every 3-4 days. For imaging, cells were grown on glass cover slips (Bellco) coated with 0.1 mg/ml poly-L-lysine and 5 µg/ml laminin from Engelbreth-Holm-Swarm murine sarcoma (Sigma).

Astrocytic culture. Primary hippocampal or mixed hippocampal/cortical astrocytic cultures were prepared from E19 or E21 embryos obtained from timed pregnant Sprague-Dawley rats (Charles River). Hippocampi and cortices were dissected as described for neuronal and mixed cultures. After digestion, tissue fragments were washed and then triturated in DMEM with GlutaMAX, 4.5 g/L glucose, and 110 mg/L sodium pyruvate supplemented with 10% heat inactivated FBS, 10 µg/mL penicillin, and 10 units/mL streptomycin. Dissociated cells were plated in 75 cm^2 flasks and cultured in a humidified atmosphere of 95% air and 5% CO_2. One week after plating (when astrocyte layer became confluent), cultures were vigorously shaken (300 rpm at 37°C) overnight to remove microglia and oligodendroglia (1); astrocytes were then washed with PBS, trypsinized, plated into 175 cm^2 tissue culture flasks, and cultured for another 1-2 weeks before being used in experiments. Cells were fed 1-2 times a week with fresh medium and passaged when confluent. Prior to experiments, cells were plated into 60 or 100 mm tissue culture dishes, 6-well tissue culture plates, or on tissue culture inserts as required.

Drugs. Sulforaphane, glutamate, bicucullin, tetrodotoxin, and nimodipine (Sigma Aldrich), 4-aminopyridine (MP Biomedicals), MG-132 (Calbiochem), BAPTA-AM, picrotoxin, gabazine, NMDA, APV, MK801, MCPG, NBQX, CNQX, DHPG and LY341495 (Tocris) were purchased in a dry (powder) form, with stock solutions prepared in either DMSO or water (as recommended by the manufacturer) and stored in small aliquots at -20°C. Drug treatments were applied in culture medium unless otherwise indicated. In pharmacology experiments, antagonists or ion channel blockers were first applied alone for 30 min and then together with the main treatment for the time indicated in figure legends. In BAPTA experiments, cultures were pretreated with

cell-permeable BAPTA-AM for 30 min, washed with medium to remove BAPTA-AM not taken up by cells, and then treated with either high K^+ or Gab/4-AP.

siRNA transfection. Astrocytes (DIV10-14) were transfected with 20-30 pmol of scrambled or Nrf2-targeting siRNA (Santa Cruz, catalog numbers SC-37007 and SC-156128 respectively) using Nucleofector II (Amaxa) according to the manufacturer's protocol. Based on separate experiments with GFP expression plasmid pmaxGFP™ (Lonza), astrocyte transfection efficiency using this approach is estimated at 70-80%.

Western blotting. Nuclear and cytoplasmic fractions were prepared using the NE-PER kit (Pierce) according to the manufacturer's instructions. The protein concentration of each sample was assayed relative to the bovine serum albumin (BSA) standard with the CBB Assay kit (Dojindo) or Quick-Start Bradford Protein Assay (Bio-Rad); 20-30 µg of protein was loaded in each lane. After solubilization with LDS sample buffer (Invitrogen) supplemented with TCEP reducing reagent (Pierce; final concentration 12 mM), samples were heated for 10 min at 70°C , electrophoretically resolved with 4-12% NuPAGE precast gels (Invitrogen), and electroblotted to nitrocellulose membranes (0.2 A for 5 hours at 4°C). 5% BSA in TBS (150 mM NaCl, 20 mM TrisCl; pH = 7.4) supplemented with 0.1% Tween (TBST) was used for dilution of primary antibodies, while 5% nonfat dried milk in TBST was used for blocking and dilution of secondary antibodies. TBST was used for all washings. For Nrf2 antibody, 5% nonfat dried milk in TBST was used for blocking, all washings and antibody dilution. Membranes were blocked for 1 h at room temperature (RT); incubated with primary antibodies for 2-3 h at RT or overnight at 4°C; washed 3 times for 30 min at RT; incubated with corresponding secondary antibody for 1 h at RT; and washed for at least 30 min at RT. Following a final wash in TBS with 0.1% Tween for 10 min at RT, protein-antibody complexes were detected using an ECL chemiluminescent kit (Pierce Biotechnology) and CL-XPosure Film (Thermo Scientific) with a Konica SRX-101A film developer. Primary antibodies included rabbit polyclonal anti-Nrf2 (H300, Santa Cruz Biotechnology; 1:400); goat polyclonal anti-laminB (C20, Santa Cruz Biotechnology; 1:200), and mouse monoclonal anti-vinculin (hVIN-1 purified immunoglobulin, Sigma; 1:5000). Secondary antibodies included goat horseradish peroxidase (HRP)-conjugated anti-rabbit secondary H+L IgG antibody (Jackson ImmunoResearch; 1:5000), bovine HRP-conjugated anti-goat secondary H+L IgG antibody (Santa Cruz Biotechnology; 1:5000), and sheep HRP-conjugated anti-mouse secondary IgG whole antibody (GE Healthcare; 1:2000).

qRT-PCR. Total RNA was isolated using RNeasy Mini Kit (Qiagen), with contaminating genomic DNA removed during the isolation by an on-column DNase digestion step; RNA concentration was measured using Nanodrop 1000. mRNA was reverse transcribed to cDNA using Cloned AMV First-Strand cDNA Synthesis Kit (Invitrogen) according to the manufacturer's instructions. qPCR reactions were carried out on CFX96 Real-Time System (Bio-Rad) using 10 ng sample in a 20 µl, 98-well format. SsoFast Probes Supermix was purchased from Bio-Rad, while TaqMan PCR primer and probe sets were purchased from Applied Biosystems for all genes tested (Nqo1: Rn00566528_m1; Gclc: Rn00563101_m1; Gclm: Rn00568900_m1; Ephx1: Rn00563349_m1; Nrf2: Rn00477784_m1). Rat ACTB Endogenous Control FAM Probe (Applied Biosystems, Rn00667869_m1) was used for normalization. The common reference cDNA, used to prepare the standard curve for all reactions, was generated by mixing total RNA from several

untreated mixed culture batches. Two technical replicates for each sample were run on one plate, with replicate plates ran for a subset of experiments to confirm accuracy. Statistical analysis was performed with GraphPad Prism statistical software using either regular two-tailed Student's t-test or two-tailed t-test with Welch's correction if variances were significantly different between control and treatment samples.

Proteasome assay. Following drug treatment, crude lysates (prepared in 0.5% NP-40 in PBS) were centrifuged at maximum speed for 10 min at 4°C to clear nuclei and non-lysed cell debris. The proteasome activity in the cleared lysates was determined using Proteasome Activity Assay Kit (BioVision, catalog #K245-100) according to the manufacturer's instructions; the fluorescence activity for each sample was measured over 60 min period using excitation and emission wavelengths of 350 and 445 nm, respectively. Fluorescence values measured at 40 min were normalized to the protein concentration determined by Quick-Start Bradford Protein Assay. For each experiment, the activity in experimental samples was normalized to the activity in the control (DMSO- or ACSF-treated) sample and statistically analyzed with GraphPad Prism statistical software using Kruskal-Wallis one-way ANOVA on ranks.

Immunocytochemistry. Neuronal, mixed or astrocytic cultures were plated on 10 mm glass coverslips. Cells were fixed [4% formaldehyde (Thermo Scientific) and 4% sucrose in PBS] for 30 min at RT, permeabilized [0.5% NP40 (Sigma) in PBS] for 30 min at RT, and blocked [5% normal goat serum (Jackson ImmunoResearch), 0.1% TritonX-100 (Fisher) in PBS] for 30 min at RT or overnight at 4°C. (Blocking solution was used for dilution of primary and secondary antibodies, while PBS with 0.1% TritonX-100 was used for washings.) After blocking, cells were incubated with mouse monoclonal anti-Map2 (clone HM-2, Sigma; 1:500) and chicken polyclonal anti-GFAP (Abcam; 1:1000) for 2 h at RT; washed 3 times for 30 min at RT; incubated with AlexaFluor 488-conjugated goat anti-rabbit IgG (Invitrogen; 1:500) and Alexa Fluor 594-conjugated goat anti chicken IgG, (Invitrogen; 1:500) for 1 h at RT; and then washed for at least 30 min at RT. Following a final wash in PBS with 0.1% TritonX-100 for 10 min at RT, cells were stained with DAPI nuclear dye and mounted using Vectashield mounting media (Vector Laboratories). Images were acquired with Eclipse C1si Spectral Confocal Microscope with EZ-C1 software (Nikon) and edited with Adobe Photoshop CS2 (version 9.0.2).

Brain slice cultures. Brain slices were obtained from homozygous or heterozygous ARE-hPAP reporter mice [(2); official strain name: B6.SJL-Tg(Nqo1-ALPP)1Jaj/Mrgt, MGI ID: 5086235]. P21-26 old mice were anesthetized with CO_2 and decapitated; brains were then quickly dissected in ice-cold SLDS. Four 400 µm-thick sections from each brain were made using a vibratome (VT1200S, Leica) in ACSF containing (in mM): 124 NaCl, 3 KCl, 1.25 KH_2PO_4, 2.5 $CaCl_2$, 2.5 $MgCl_2$, 26 $NaHCO_3$, 10 glucose, and 2 ascorbic acid. Slices were placed onto cell culture inserts (BD Falcon or Millipore) in 6-well plates and kept in a culture medium containing (by volume): 66% Basal Medium Eagle (BME), 25% Hanks Balanced Salt Solution (BSS), 5% FBS, 1% N2 supplement, 1% penicillin/streptomycin/glutamine and 0.66% glucose (3). Cultures were maintained in a humidified incubator at 37°C with constant 5% CO_2 supply overnight for recovery. For next 48 h, four slices from one animal were treated as one set with vehicle (0.1% DMSO), 2.5 µM SLF, 20 µM Gab + 2.5 mM 4-AP (to induce neuronal firing), or 20 µM Gab + 2.5 mM 4-AP + 1 µM TTX (to block neuronal firing).

hPAP histochemistry. Slices were fixed in 4% paraformaldehyde in PBS for 20 min at RT. Fixed slices were cryoprotected (in 15% sucrose for 4 h followed by 30% sucrose overnight), snap-frozen in 1:1 mixture of 30% sucrose and OCT tissue freezing medium (Tissue-Tek), and cut into 20 µM-thick sections on a cryostat. Frozen sections were rehydrated in a 50 mM Tris-5 mM magnesium saline solution (TMN) for 15 min at RT, followed by incubation in TMN at 65°C for 20 min to heat inactivate endogenous alkaline phosphatase activity. Sections were then stained by replacing TMN with a staining solution containing 0.33 mg/mL of nitro blue tetrazolium (NBT; Promega) and 0.165 mg/mL 5-bromo-4-chloro-3-indoly-phosphate (BCIP; Promega) and incubating at 37°C for 55 min (2). After washing with PBS, sections were counterstained with Fast Red (Vector Laboratories) and mounted in Fluoromount-G (Cell Lab) for quantification. A subset of sections went through a dehydration process (75% ethanol, 90% ethanol, 100% ethanol, 100% ethanol, xylene) and mounting in Mounting Medium (Richard-Allan Scientific) for micro-photography; images were taken with a DP72 camera on BX41 bright-field microscope using cellSense Entry 1.6 software (all by Olympus) and were edited with Adobe Photoshop CS5 Version 12.1.32.

Quantification of hPAP-positive astrocytes. hPAP-positive cells with astrocyte morphology, displaying both bushy processes and well-defined cell bodies, were counted under low magnification from the entire section area; the cell counts were averaged over 4-8 sections from each slice. For each experimental set (4 slices from one animal, each exposed to one of the four treatments described above), the data were normalized to the cell count in the vehicle-treated slice and analyzed with GraphPad Prism statistical software using Kruskal-Wallis one-way ANOVA on ranks.

Electrophysiology. P21 homozygous or heterozygous ARE-hPAP mice were anesthetized with CO_2 and decapitated; brains were then quickly dissected in ice-cold ACSF and acute transverse 300 µM thick neocortical slices were prepared using a vibratome (VT1200S, Leica). Oxygenation (95% O_2/5% CO_2) was continuously supplied during slice sectioning, recovery, and recording. After recovery at RT for 45 min in ACSF, whole-cell current-clamp recordings of neocortical pyramidal neurons were performed with a Multiclamp 700B amplifier (Molecular Devices). Signals were filtered at 1 kHz and sampled at 10 kHz using a Digidata 1440A analog-to-digital converter (Molecular Devices). All data were recorded and analyzed with pClamp 10 software (Molecular Devices). Patch electrodes (3-4 MΩ) contained (in mM) 115 K-gluconate, 20 KCl, 10 Na_2phosphate, 10 HEPES, 2 Mg_3ATP, and 0.3 Na_2GTP (~ 290 mOsm; pH 7.4). Spontaneous action potentials were recorded at 0 mV; action potential frequency before and after Gab/4-AP or SLF treatment was determined by manually counting the number of spikes over 50-100 s and statistically analyzed with GraphPad Prism statistical software using two-tailed paired t-test.

1. McCarthy KD, de Vellis J (1980) Preparation of separate astroglial and oligodendroglial cell cultures from rat cerebral tissue. *J Cell Biol* 85:890-902.
2. Johnson DA, Andrews GK, Xu W, Johnson JA (2002) Activation of the antioxidant response element in primary cortical neuronal cultures derived from transgenic reporter mice. *J Neurochem* 81:1233-1241.
3. Wang X, Tsai JW, LaMonica B, Kriegstein AR (2011) A new subtype of progenitor cell in the mouse embryonic neocortex. *Nat Neurosci* 14:555-561.

Supplemental Figure Legends

Fig. S1. Antibody specificity and specificity / time course of treatments. (A) To evaluate anti-Nrf2 antibody specificity, astrocytes were transfected with 20 pmol of either scrambled or Nrf2-targeting siRNA one day prior to overnight treatment with 0.1% DMSO (Veh) or 2.5 µM SLF. While anti-Nrf2 antibody detected multiple bands, only the band with apparent molecular weight of 84 kDa (arrow, top panel) was increased by SLF treatment and attenuated by Nrf2 siRNA transfection; the other bands were nonspecific. (Apparent MW of 84 kDa was measured following electrophoresis in precast Invitrogen gels; in gels cast in our lab, the Nrf2 band ran at apparent MW of 98 kDa.) **(B)** Mixed cultures were treated with 0.1% DMSO (Veh), 2.5 µM SLF, 20 µM Gab, 2.5 mM 4-AP, or 20 µM Gab + 2.5 mM 4-AP (Gab/4-AP) for 24 h. Nuclear Nrf2 protein level was increased to a larger extent by the combined Gab/4-AP treatment than by separate Gab and 4-AP treatments, indicating additive effect. A representative of 3 similar experiments is shown. **(C and D)** Neuronal, mixed and astrocytic cultures were treated with 0.1% DMSO (Veh) for 24 h, 30 µM bicuculline (Bic) + 2.5 mM 4-AP (C) or 30 µM picrotoxin (PcTX) + 2.5 mM 4-AP (D) for 24 h, or 2.5 µM SLF for 16 h (C and D). As with Gab/4-AP treatment (Fig. 1C), nuclear Nrf2 protein level was increased by Bic/4-AP or PcTX/4-AP treatments only in mixed cultures. **(E and F)** Mixed cultures were treated as described in Fig.1C legend for 6, 16 or 24 h (E); neuronal, mixed, or astrocytic cultures were treated as described in Fig. 1B legend for 2 or 6 h (F). In mixed cultures, nuclear Nrf2 protein level was increased by Gab/4-AP after 16 and 24 h (E) and by high K^+ after 2 and 6 h (F).

Fig. S2. Activation of Nrf2-dependent genes in predominantly neuronal cultures. Predominantly neuronal cultures were treated with control or high K^+ ACSF for 4 h **(A)** or with 0.1% DMSO (Veh) or Gab/4-AP for 24 h **(B)**. A statistically significant increase in Nqo1 mRNA was seen with both treatments, while Ephx1 mRNA was increased only after high K^+ treatment and Gclc mRNA only after Gab/4-AP treatment; the level of Gclm mRNA was not significantly changed in either experiment. Note that the absolute level of each mRNA (except Gclm), both before and after treatment, was lower in predominately neuronal than in mixed cultures (compare this figure with Figs. 1D and 1E), suggesting that these mRNAs were largely derived from non-neuronal cells in both culture types. *, $p<0.05$; **, $p<0.01$; ***, $p<0.001$ (mean±SEM; t-test, n=4).

Fig. S3. Co-culturing neurons and astrocytes for 24 h is sufficient for Nrf2 pathway activation by high K^+ and Gab/4-AP. Direct neuron-astrocyte co-cultures were obtained by plating astrocytes into DIV14 neuronal cultures; experiments were performed 24 h following astrocyte plating. Cultures were treated as described in Fig. 1 legend. Nuclear Nrf2 protein level was increased by high K^+ and Gab/4-AP treatments to a similar extent in mixed and direct neuron-astrocyte co-cultures, as seen when neurons and astrocytes were co-cultured for 6 days (Fig. 2).

Fig. S4. Gab/4-AP treatment, but not SLF treatment, increases neuronal firing frequency in brain slices from hPAP reporter mice. (A) Representative traces from a single cortical neuron treated first with 0.1% DMSO (Veh; top) and then with 20 µM Gab + 2.5 mM 4-AP (Gab/4-AP; bottom) in ACSF; each spike corresponds to a single action potential. **(B)** The

increase in action potential frequency induced by Gab/4-AP treatment was statistically significant (**, p<0.01; paired t-test, n=6). **(C)** Representative traces from a single cortical neuron treated first with 0.1% DMSO (Veh; top) and then with 2.5 µM SLF (bottom) in ACSF; each spike corresponds to a single action potential. **(D)** SLF treatment did not result in a statistically significant change in action potential frequency (paired t-test, n=5).

Fig. S5. In neuron-astrocyte co-cultures, increase in Nrf2 nuclear level is attenuated by Nrf2 knock-down in astrocytes. Direct neuron-astrocyte co-cultures were obtained by plating astrocytes transfected with 30 pmol of either scrambled or Nrf2-targeting siRNA into DIV15 neuronal cultures; drug treatments (as described in Fig. 1 legend) were performed 24 h following astrocyte plating. Increase in nuclear Nrf2 protein level induced by Gab/4-AP and high K^+ treatments was attenuated when astrocytes were transfected by Nrf2 siRNA, confirming that neuronal activity regulates astrocytic Nrf2 signaling. Like the experiment shown in Fig. S1A, this experiment demonstrates that only 84 kDa band corresponds to Nrf2, while the other bands recognized by anti-Nrf2 antibody are nonspecific. Please note that the blot on the right side of the figure is shown at a shorter exposure to avoid saturation of strong SLF signals; hence, the two nonspecific bands running at ~ 37 kDa are not visible. A representative of 3 repeat experiments is shown.

Fig. S6. Nrf2 activation by Gab/4-AP, but not high K^+, is restricted to mature cultures. Mixed cultures were treated as described in Fig. 1 legend at DIV3, DIV7, or DIV14. Compared to vehicle treatment, Gab/4-AP treatment increased nuclear Nrf2 protein level only in DIV14 cultures **(A)**, while high K^+ treatment led to Nrf2 activation at all culture ages tested **(B)**. Representative of 3 similar experiments are shown.

Fig. S7. Nrf2 activation depends on glutamate receptor signaling and requires extracellular Ca^{2+}. (A) Mixed cultures were treated as described in Fig. 4A legend. In this experiment, NBQX and CNQX attenuated Nrf2 activation by Gab/4-AP to a lesser extent than in experiment shown in Fig. 4A. **(B)** Mixed cultures were pre-treated with 50 µM BAPTA-AM for 30 min, washed, and then treated with Gab/4-AP for 24 h; sister cultures were treated as described in Fig. 4A legend. Increase in Nrf2 nuclear level induced by Gab/4-AP treatment was blocked by both EGTA and BAPTA, but interpretation of BAPTA experiment is complicated by the neurotoxicity of long (24 h) chelation of intracellular Ca^{2+}. A representative of 3 similar experiments is shown. **(C)** Mixed cultures were treated as described in Fig. 4B legend, except that high K^+, 0 Ca^{2+} ACSF (97.25 mM NaCl, 50 mM KCl, 1 mM $MgCl_2$, 10 mM HEPES-NaOH, 2.5 mM EGTA-NaOH, 10 mM glucose; pH 7.4) was used as one of the treatments. In this experiment, MK801 (but not APV) partly blocked Nrf2 activation by high K^+ treatment; this outcome was seen only rarely (in 3 of 10 experiments). APV was consistently without an effect (4 of 4 experiments). **(D)** Astrocytes were treated as described in Fig. 4C legend. Nuclear Nrf2 protein level was increased following treatment by glutamate or mGluR group 1 agonist DHPG, but not NMDA; this effect was blocked by Ca^{2+} chelator EGTA. This outcome was seen in 2 of 6 experiments; the remaining 4 experiments showed no increase in nuclear Nrf2 following treatment by glutamate receptor agonists (Fig. 4C).

Fig. S8. The effect of high K^+ and Gab/4-AP treatments on Nrf2 mRNA level and proteasome activity. Mixed (A and C) or astrocytic cultures (B) were treated with control or high K^+ ACSF for 4-6 h or with 0.1% DMSO (Veh), 2.5 µM SLF, or Gab/4-AP in the culture medium for 24 h. **(A)** In mixed cultures, a statistically significant increase in Nrf2 mRNA was seen with both high K^+ (left) and Gab/4-AP treatments (right); SLF treatment had no effect. (**, $p<0.01$; ****, $p<0.0001$; mean±SEM; t-test [left] or one-way ANOVA [right], n=4-5) **(B)** In astrocytic cultures, high K^+ treatment (left) led to a statistically significant increase in Nrf2 mRNA; however, the degree of change was much smaller than in mixed cultures (60% increase vs. 700% increase; compare with A). In contrast, there was no increase in Nrf2 mRNA level following SLF or Gab/4-AP treatments (right). (***, $p<0.001$; mean±SEM; t-test [left] or one-way ANOVA [right], n=4-5) Note that in mixed cultures (A), but not in astrocytic cultures (B), baseline Nrf2 mRNA level was lower in ACSF than in the culture medium (which was used for SLF and Gab/4-AP treatments). **(C)** 2.5 µM SLF and 1 µM MG-132 (proteasome inhibitor used as a positive control) were applied in control ACSF for 4 h (left) or in culture medium for 24 h (right). Proteasome activity was not significantly altered by SLF, high K^+ or Gab/-4-AP treatments. Proteasome inhibition induced by MG-132 treatment was statistically significant ($p<0.05$) in experiment shown on the right but not in the experiment shown on the left, reflecting greater experimental variability associated with the shorter length of treatment (4 h vs. 24 h) in ACSF than the culture medium. Each symbol denotes a separate experiment (n=4-5; Kruskal-Wallis ANOVA on ranks).

Figure 1

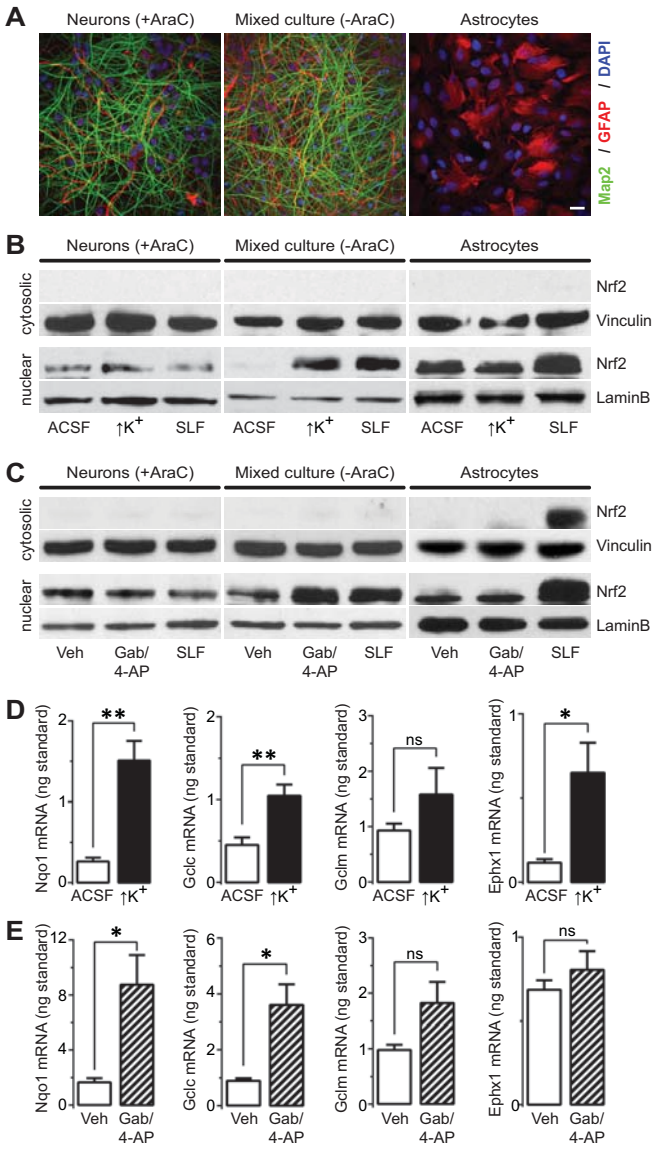
A
Neurons (+AraC)
Mixed culture (-AraC)
Astrocytes
Map2 / GFAP / DAPI
B
Neurons (+AraC)
Mixed culture (-AraC)
Astrocytes
cytosolic
nuclear
Nrf2
Vinculin
Nrf2
LaminB
ACSF
↑K+
SLF
C
Neurons (+AraC)
Mixed culture (-AraC)
Astrocytes
cytosolic
nuclear
Nrf2
Vinculin
Nrf2
LaminB
Veh
Gab/ 4-AP
SLF
D
Nqo1 mRNA (ng standard)
Gclc mRNA (ng standard)
Gclm mRNA (ng standard)
Ephx1 mRNA (ng standard)
**
**
ns
*
ACSF
↑K+
E
Nqo1 mRNA (ng standard)
Gclc mRNA (ng standard)
Gclm mRNA (ng standard)
Ephx1 mRNA (ng standard)
*
*
ns
ns
Veh
Gab/ 4-AP

Figure 2

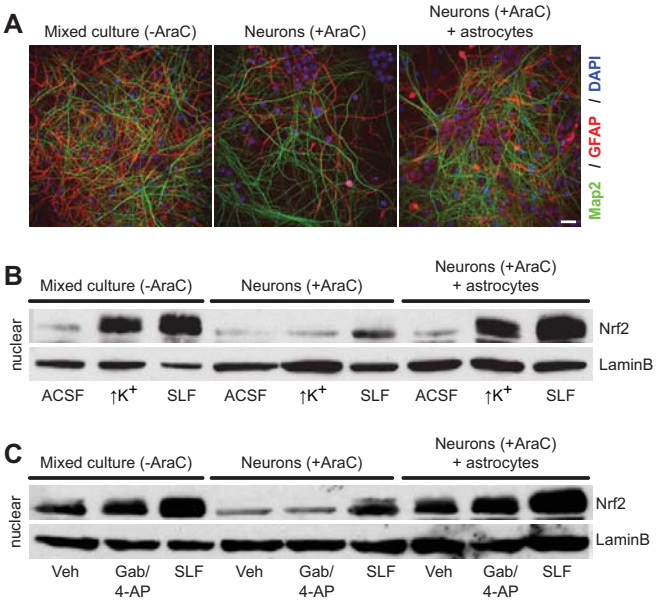
A
Mixed culture (-AraC)
Neurons (+AraC)
Neurons (+AraC)
+ astrocytes
Map2 / GFAP / DAPI
B
Mixed culture (-AraC)
Neurons (+AraC)
Neurons (+AraC)
+ astrocytes
nuclear
Nrf2
LaminB
ACSF
↑K+
SLF
ACSF
↑K+
SLF
ACSF
↑K+
SLF
C
Mixed culture (-AraC)
Neurons (+AraC)
Neurons (+AraC)
+ astrocytes
nuclear
Nrf2
LaminB
Veh
Gab/
4-AP
SLF
Veh
Gab/
4-AP
SLF
Veh
Gab/
4-AP
SLF

Figure 3

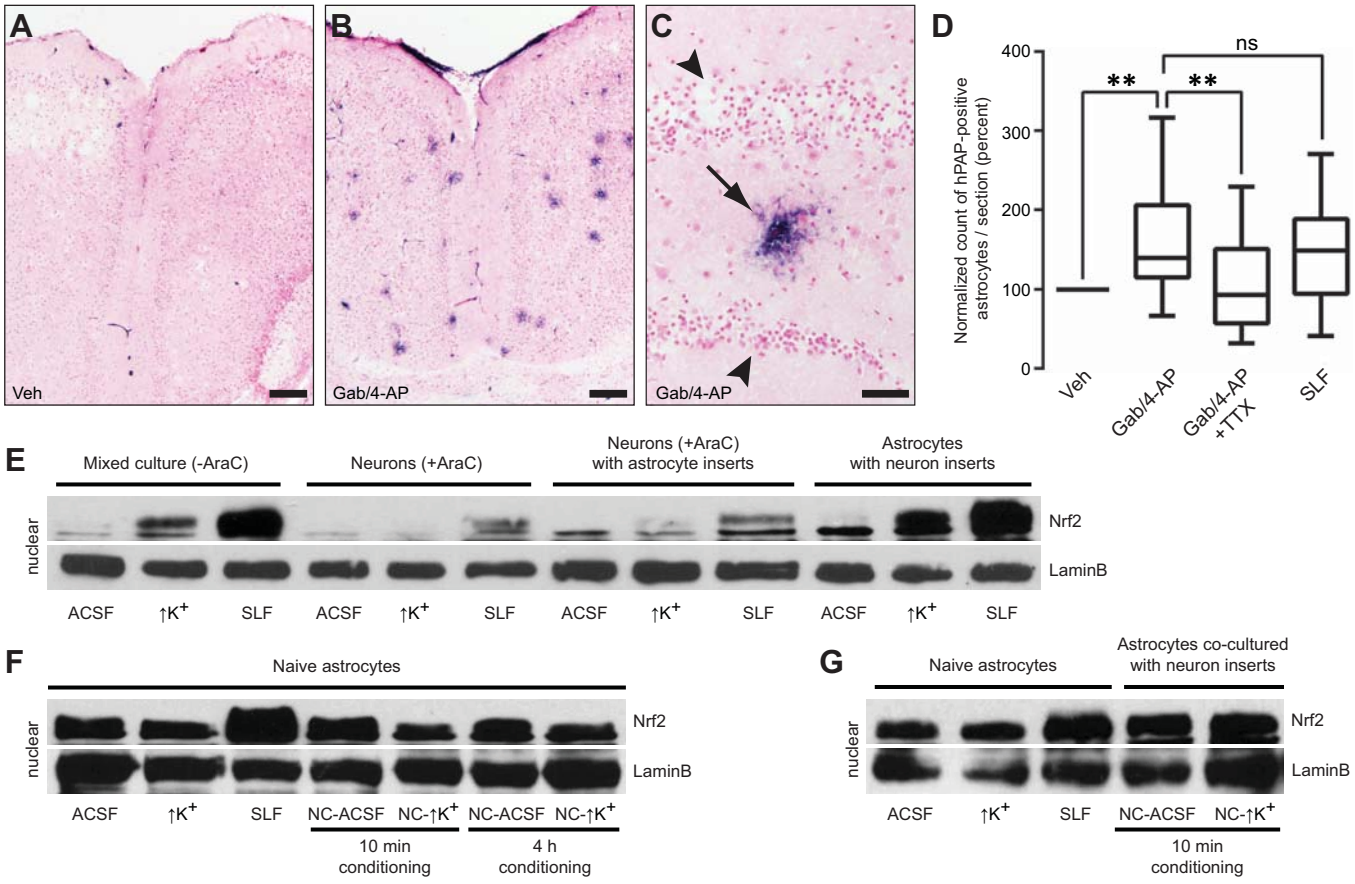
A
Veh
B
Gab/4-AP
C
Gab/4-AP
D
Normalized count of hPAP-positive astrocytes / section (percent)
400
300
200
100
0
**
**
ns
Veh
Gab/4-AP
Gab/4-AP +TTX
SLF
E
Mixed culture (-AraC)
Neurons (+AraC)
Neurons (+AraC) with astrocyte inserts
Astrocytes with neuron inserts
nuclear
Nrf2
LaminB
ACSF
↑K+
SLF
F
Naive astrocytes
nuclear
Nrf2
LaminB
ACSF
↑K+
SLF
NC-ACSF
NC-↑K+
10 min conditioning
4 h conditioning
G
Naive astrocytes
Astrocytes co-cultured with neuron inserts
nuclear
Nrf2
LaminB
ACSF
↑K+
SLF
NC-ACSF
NC-↑K+
10 min conditioning

Figure 4

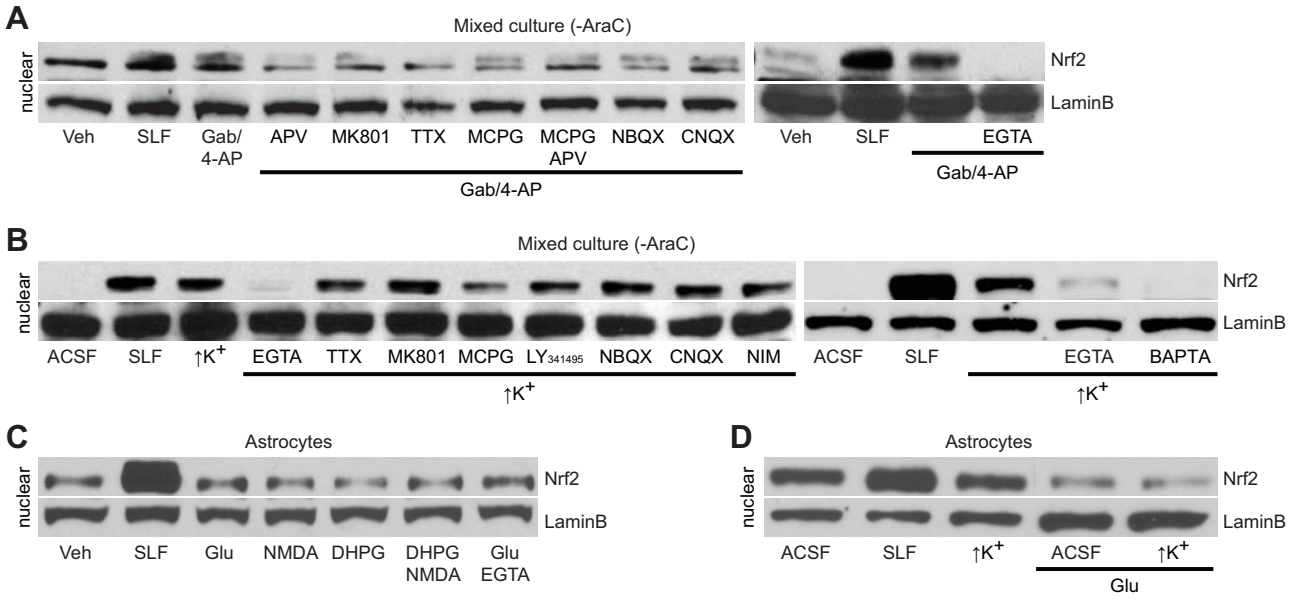
A
Mixed culture (-AraC)
nuclear
Nrf2
LaminB
Veh
SLF
Gab/ 4-AP
APV
MK801
TTX
MCPG
MCPG APV
NBQX
CNQX
Gab/4-AP
Veh
SLF
EGTA
Gab/4-AP
B
Mixed culture (-AraC)
nuclear
Nrf2
LaminB
ACSF
SLF
↑K+
EGTA
TTX
MK801
MCPG
LY341495
NBQX
CNQX
NIM
↑K+
ACSF
SLF
EGTA
BAPTA
↑K+
C
Astrocytes
nuclear
Nrf2
LaminB
Veh
SLF
Glu
NMDA
DHPG
DHPG NMDA
Glu EGTA
D
Astrocytes
nuclear
Nrf2
LaminB
ACSF
SLF
↑K+
ACSF
↑K+
Glu

Figure 5

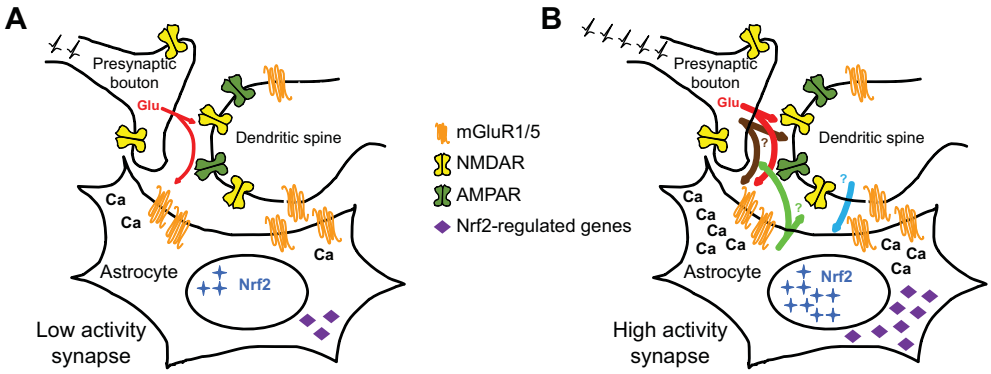
A
Presynaptic bouton
Glu
Dendritic spine
Ca
Ca
Ca
Astrocyte
Nrf2
Low activity synapse
mGluR1/5
NMDAR
AMPAR
Nrf2-regulated genes
B
Presynaptic bouton
Glu
Dendritic spine
Ca
Ca
Ca
Ca
Ca
Ca
Ca
Ca
Astrocyte
Nrf2
High activity synapse

Figure S1

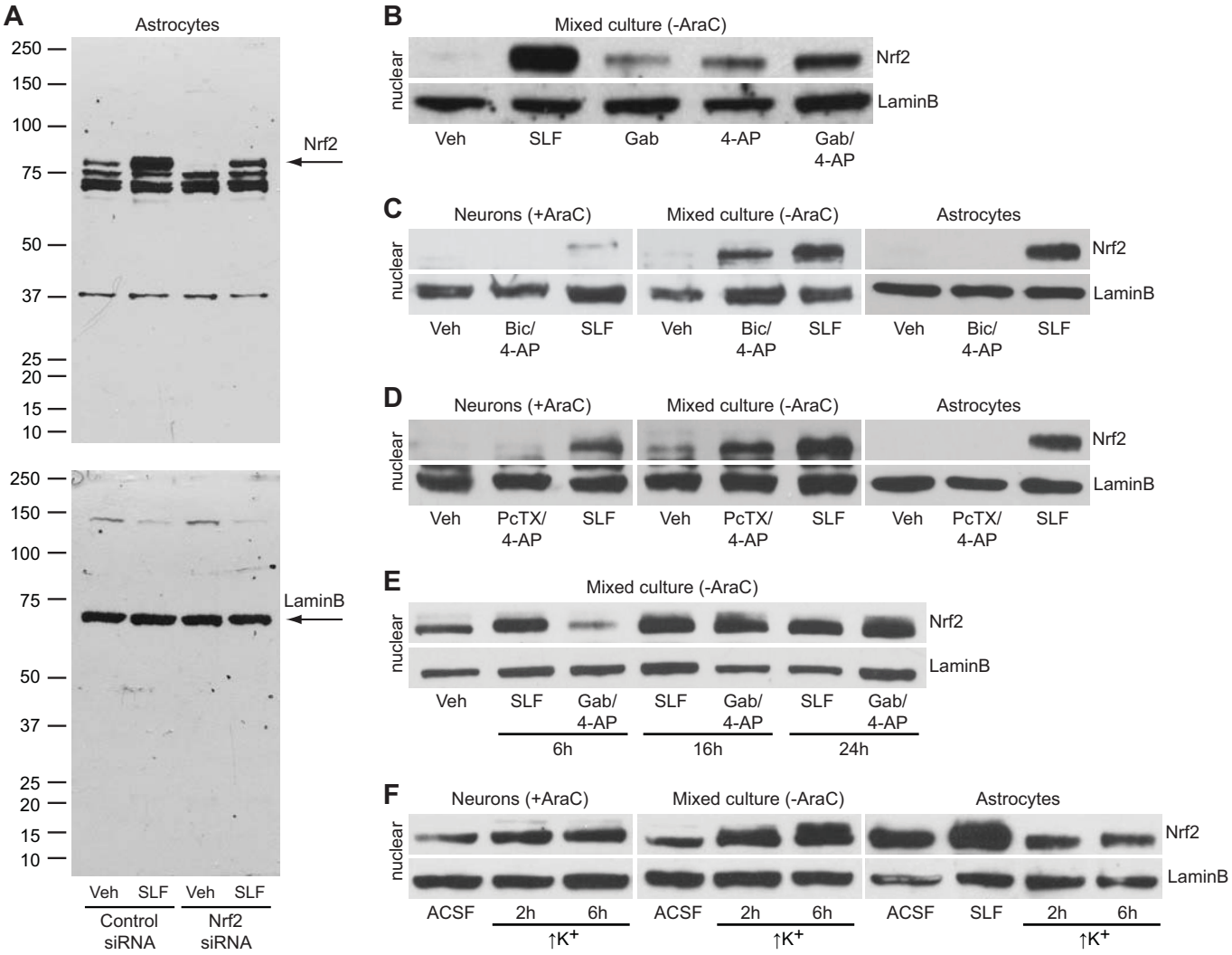
A
Astrocytes
250
150
100
75
50
37
25
20
15
10
Nrf2
LaminB
Veh
SLF
Veh
SLF
Control siRNA
Nrf2 siRNA
B
Mixed culture (-AraC)
nuclear
Nrf2
LaminB
Veh
SLF
Gab
4-AP
Gab/ 4-AP
C
Neurons (+AraC)
Mixed culture (-AraC)
Astrocytes
nuclear
Nrf2
LaminB
Veh
Bic/ 4-AP
SLF
D
Neurons (+AraC)
Mixed culture (-AraC)
Astrocytes
nuclear
Nrf2
LaminB
Veh
PcTX/ 4-AP
SLF
E
Mixed culture (-AraC)
nuclear
Nrf2
LaminB
Veh
SLF
Gab/ 4-AP
6h
16h
24h
F
Neurons (+AraC)
Mixed culture (-AraC)
Astrocytes
nuclear
Nrf2
LaminB
ACSF
2h
6h
SLF
↑K+

Figure S2

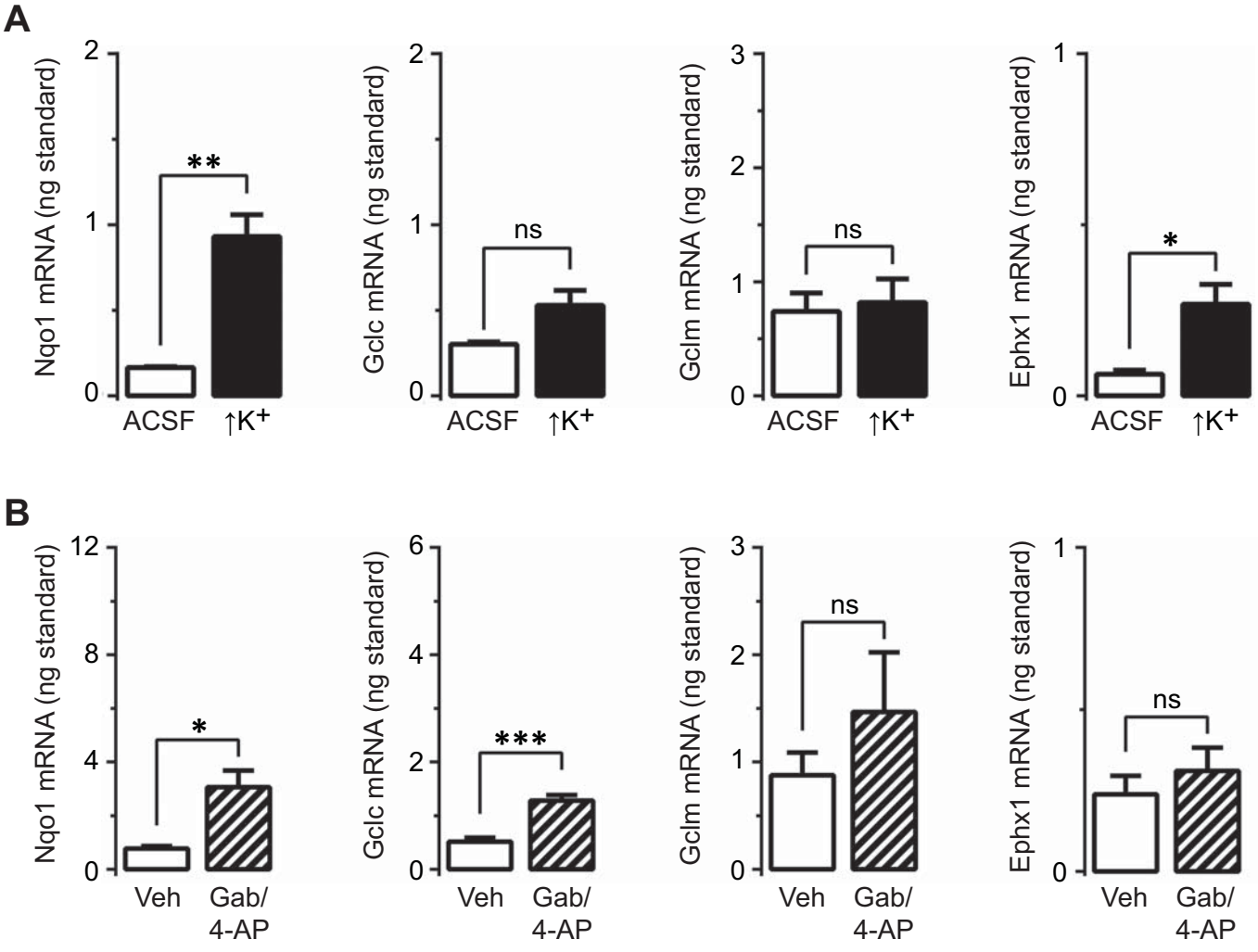
A
Nqo1 mRNA (ng standard)
Gclc mRNA (ng standard)
Gclm mRNA (ng standard)
Ephx1 mRNA (ng standard)
**
ns
ns
*
ACSF
↑K+
B
Nqo1 mRNA (ng standard)
Gclc mRNA (ng standard)
Gclm mRNA (ng standard)
Ephx1 mRNA (ng standard)
*
***
ns
ns
Veh
Gab/
4-AP

Figure S3

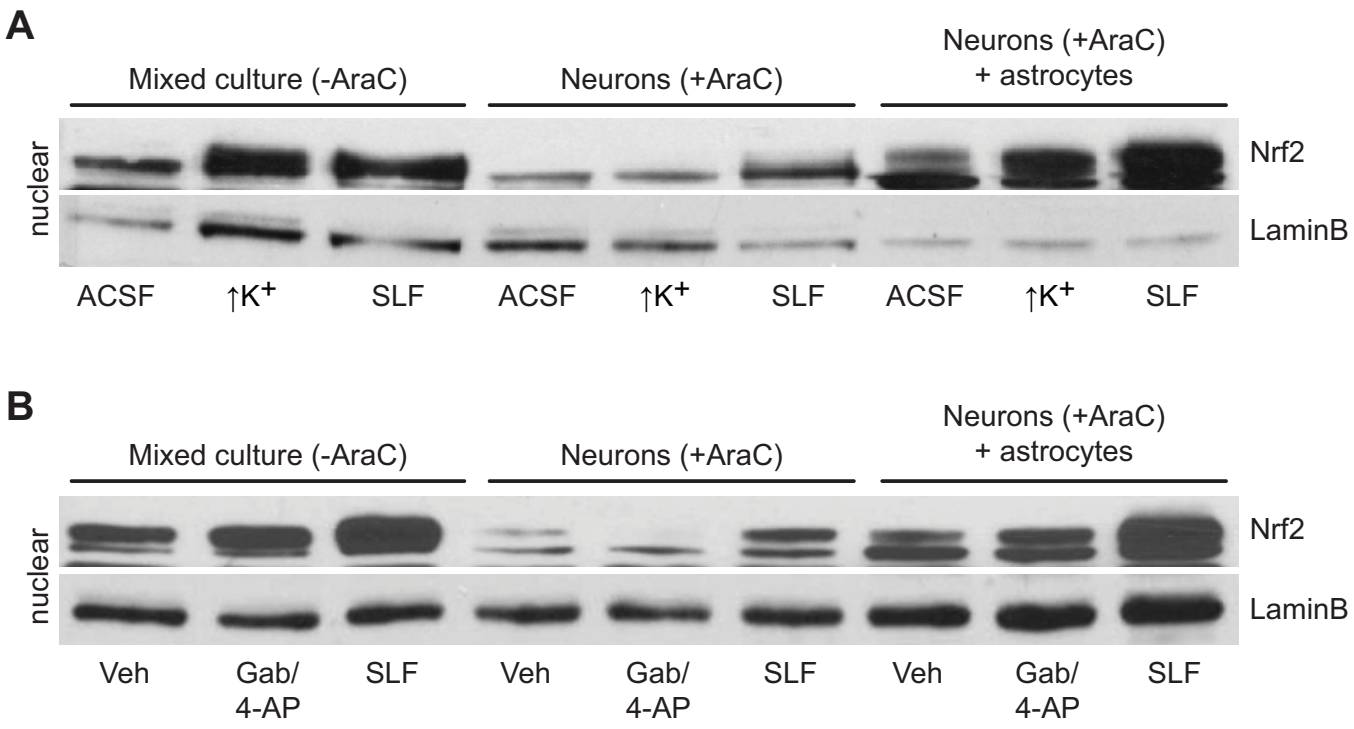
A
Mixed culture (-AraC)
Neurons (+AraC)
Neurons (+AraC)
+ astrocytes
nuclear
Nrf2
LaminB
ACSF
↑K+
SLF
ACSF
↑K+
SLF
ACSF
↑K+
SLF
B
Mixed culture (-AraC)
Neurons (+AraC)
Neurons (+AraC)
+ astrocytes
nuclear
Nrf2
LaminB
Veh
Gab/
4-AP
SLF
Veh
Gab/
4-AP
SLF
Veh
Gab/
4-AP
SLF

Figure S4

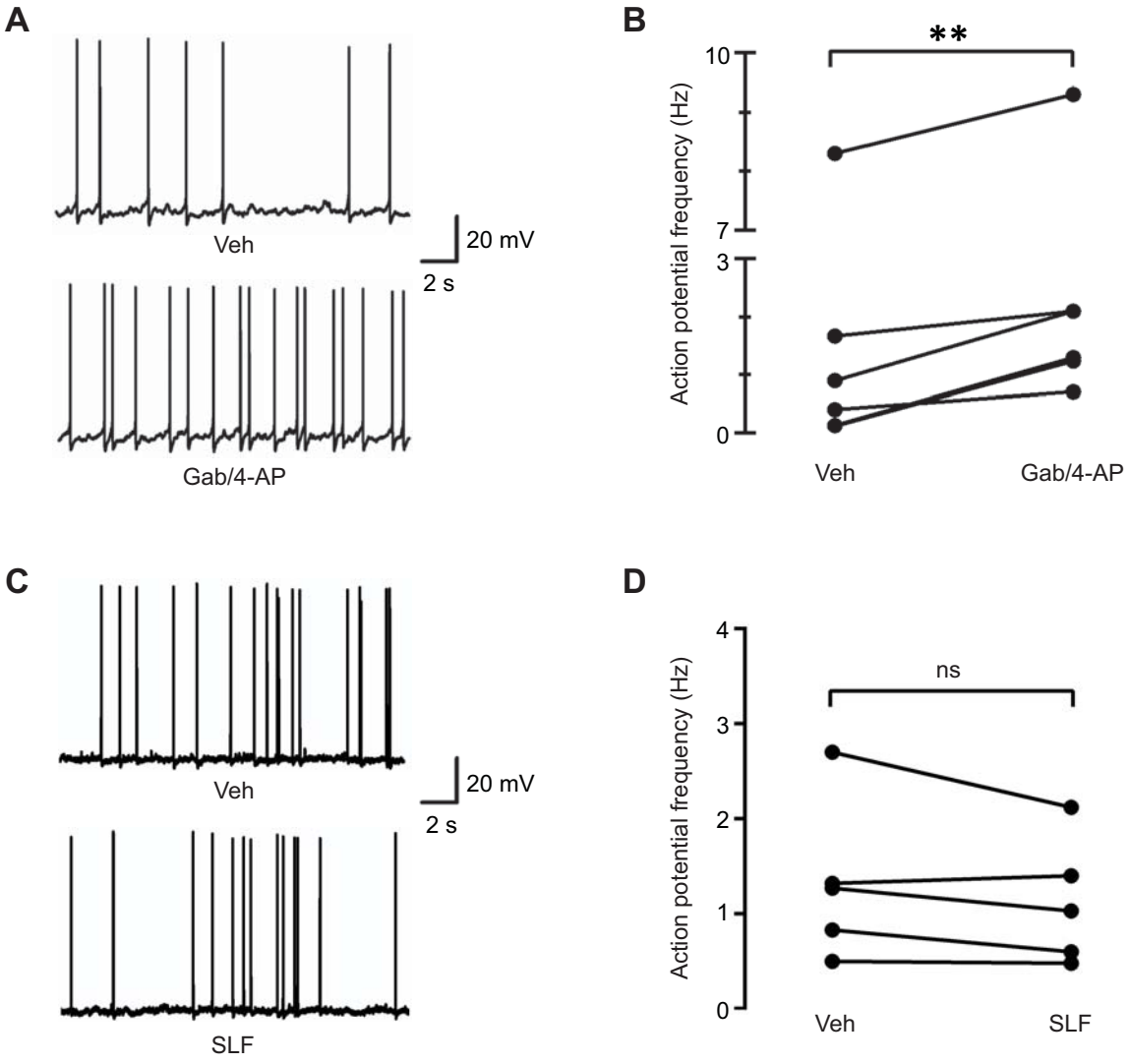
A
Veh
20 mV
2 s
Gab/4-AP
B
**
10
7
3
0
Action potential frequency (Hz)
Veh
Gab/4-AP
C
Veh
20 mV
2 s
SLF
D
ns
4
3
2
1
0
Action potential frequency (Hz)
Veh
SLF

Figure S5

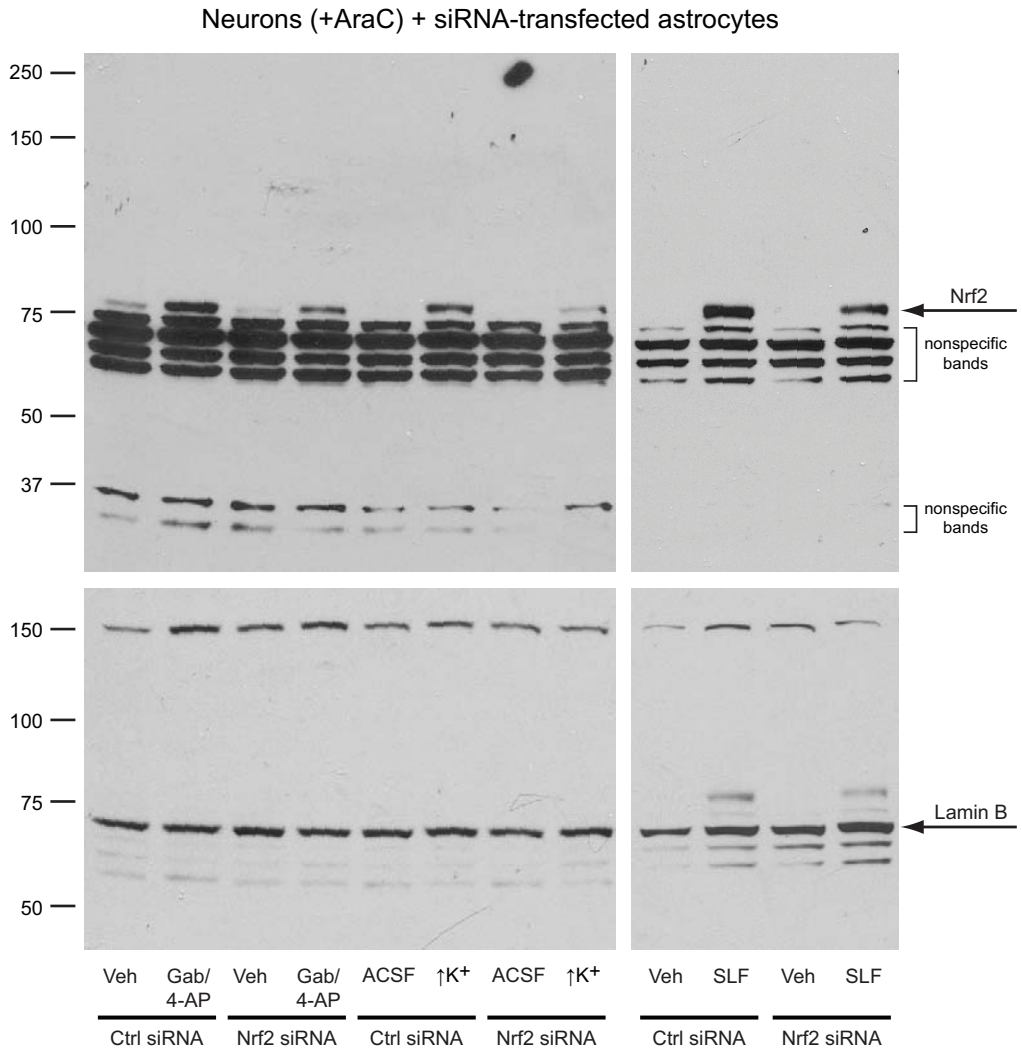
Neurons (+AraC) + siRNA-transfected astrocytes
250
150
100
75
50
37
Nrf2
nonspecific bands
nonspecific bands
150
100
75
50
Lamin B
Veh
Gab/ 4-AP
Veh
Gab/ 4-AP
ACSF
↑K+
ACSF
↑K+
Veh
SLF
Veh
SLF
Ctrl siRNA
Nrf2 siRNA
Ctrl siRNA
Nrf2 siRNA
Ctrl siRNA
Nrf2 siRNA

Figure S6

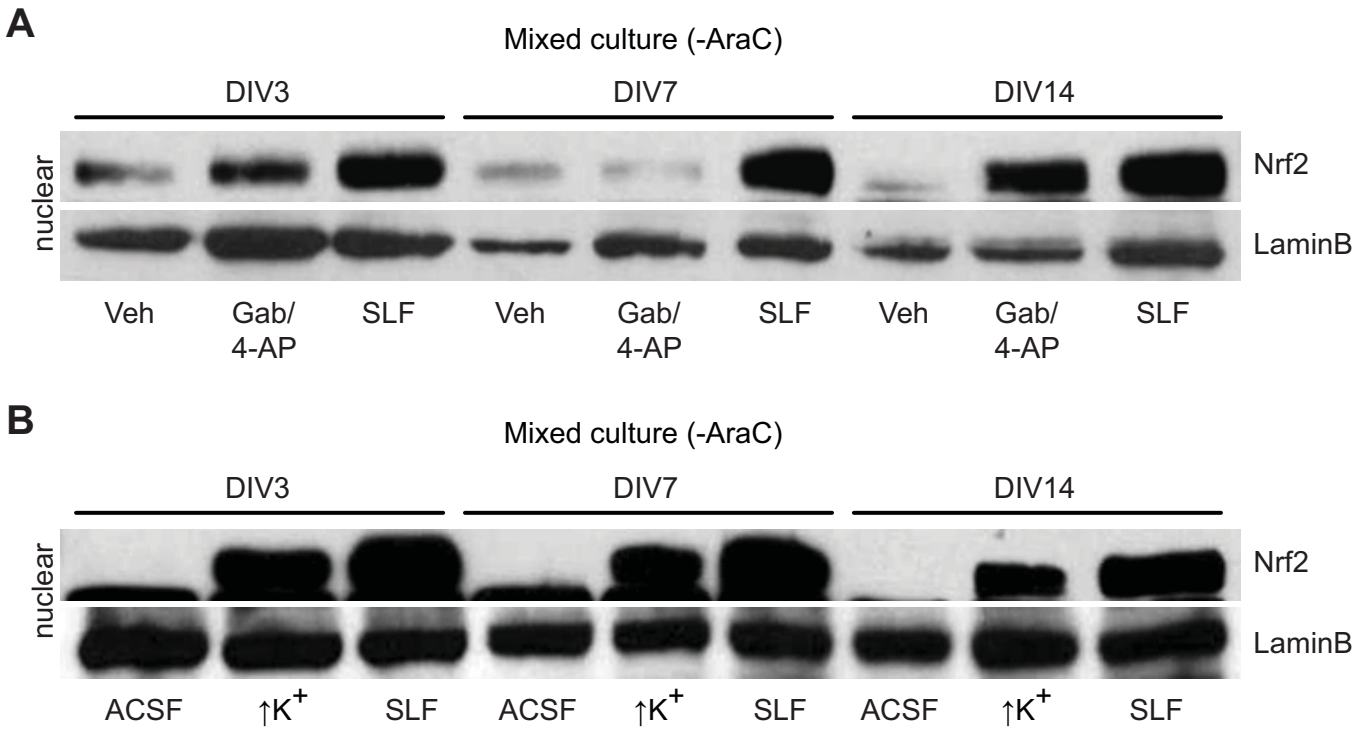
A
Mixed culture (-AraC)
DIV3
DIV7
DIV14
nuclear
Nrf2
LaminB
Veh
Gab/ 4-AP
SLF
Veh
Gab/ 4-AP
SLF
Veh
Gab/ 4-AP
SLF
B
Mixed culture (-AraC)
DIV3
DIV7
DIV14
nuclear
Nrf2
LaminB
ACSF
↑K+
SLF
ACSF
↑K+
SLF
ACSF
↑K+
SLF

Figure S7

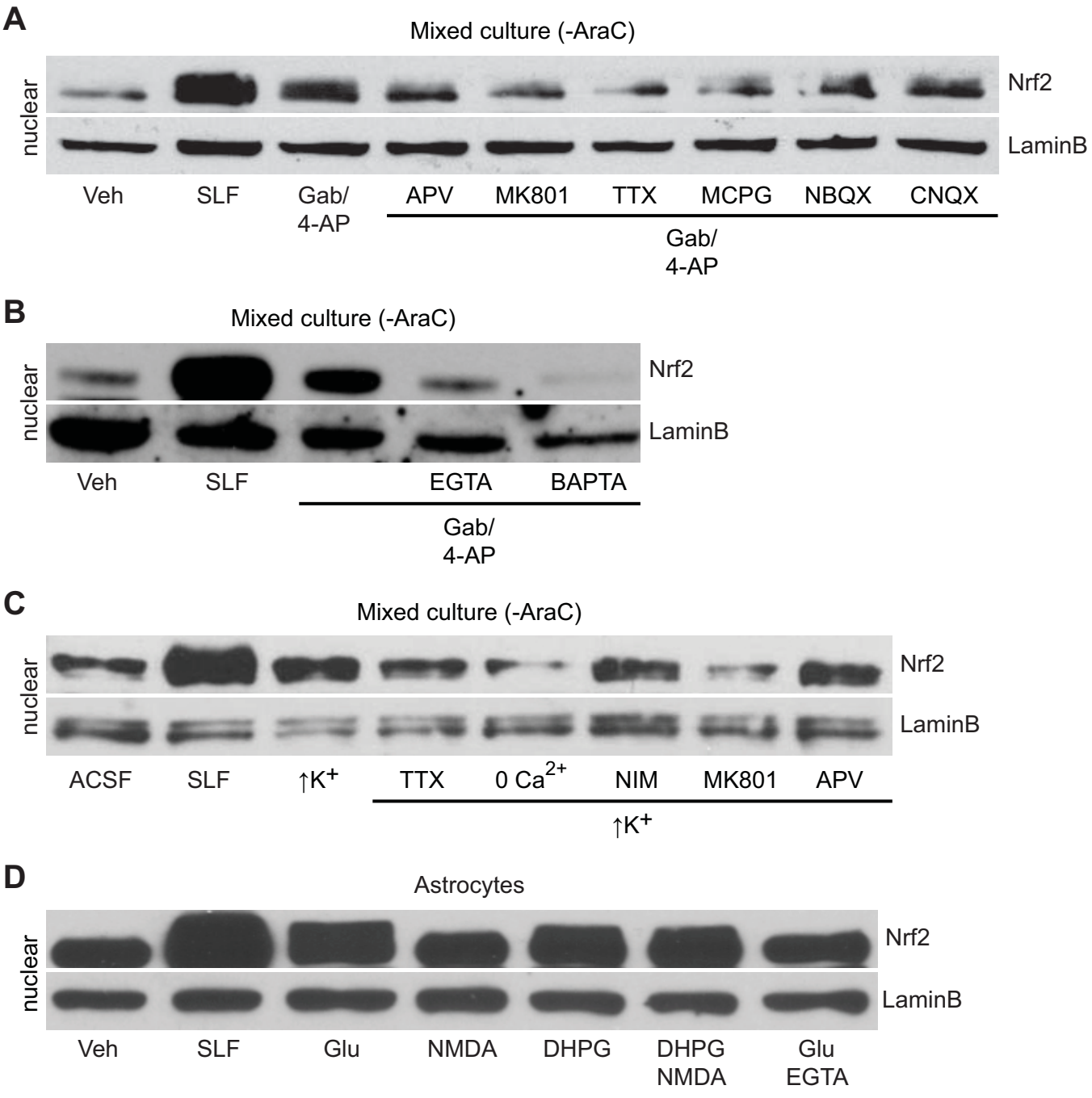
A
Mixed culture (-AraC)
nuclear
Nrf2
LaminB
Veh
SLF
Gab/
4-AP
APV
MK801
TTX
MCPG
NBQX
CNQX
Gab/
4-AP
B
Mixed culture (-AraC)
nuclear
Nrf2
LaminB
Veh
SLF
EGTA
BAPTA
Gab/
4-AP
C
Mixed culture (-AraC)
nuclear
Nrf2
LaminB
ACSF
SLF
↑K+
TTX
0 Ca2+
NIM
MK801
APV
↑K+
D
Astrocytes
nuclear
Nrf2
LaminB
Veh
SLF
Glu
NMDA
DHPG
DHPG
NMDA
Glu
EGTA

Figure S8

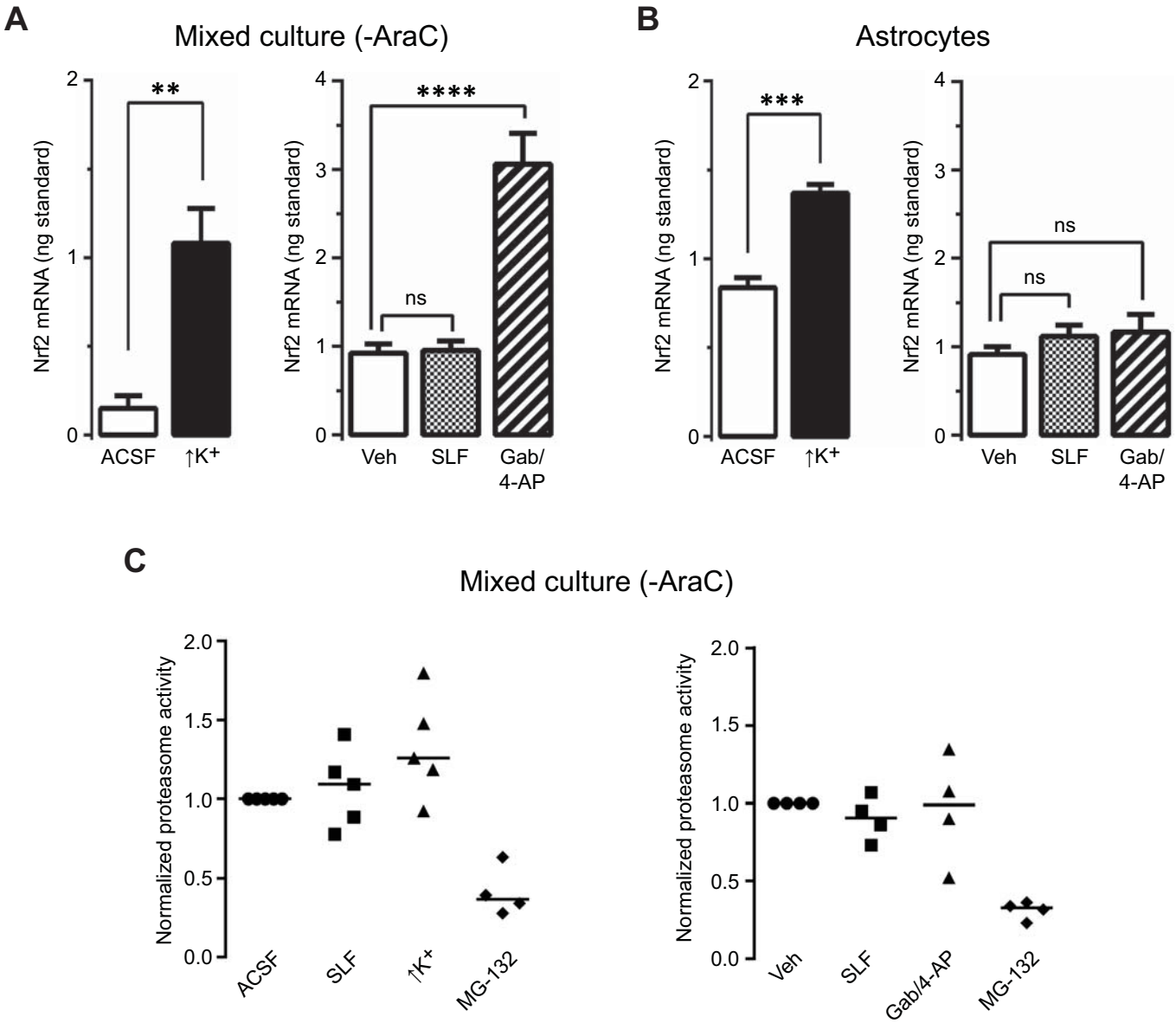
A
Mixed culture (-AraC)
Nrf2 mRNA (ng standard)
**
ACSF
↑K+
****
ns
Veh
SLF
Gab/
4-AP
B
Astrocytes
***
ns
ns
C
Mixed culture (-AraC)
Normalized proteasome activity
MG-132
Gab/4-AP